Figure 3. CD10 and sphere formation. (A–B) CD10 expression in sphere cells was compared with that of adherent (control) cells in FaDu and Detroit562 by flow cytometry. (C) CD10(+) and CD10(−) cells were sorted and the morphology of spheroid colonies in FaDu were examined. Representative images are shown. (D–E) The number of spheroid colonies formed in CD10(+)/(−) FaDu (D) and Detroit562 (E) were calculated. (F–G) The sizes of spherical colonies of CD10(+)/(−) in FaDu (F) and Detroit562 (G) were also determined. Data represent means ± s.e.m.; $*P < 0.05$; $**P < 0.01$.

Table 2. Tumourigenicity of CD10(+) and CD10(−) Detroit562 cells		
No. of cells used for inoculation	No. of tumours from CD10(+) cells	No. of tumours from CD10(−) cells
10 000	4/4	4/4
1000	6/6	2/6
100	1/4	0/4

Second, it is the difference of products of antibodies such as clone number, type of fluorophores and method of staining. These may further underlie differences in technical sensitivity. However, both techniques clearly demonstrated that CD10 was upregulated in response to either cisplatin or radiation treatment, as well as in the cisplatin-resistant cell line.

CD10, also known as membrane metalloendopeptidase, neutral endopeptidase, neprilysin and common acute lymphoblastic leukaemia antigen (CALLA), is a zinc-dependent
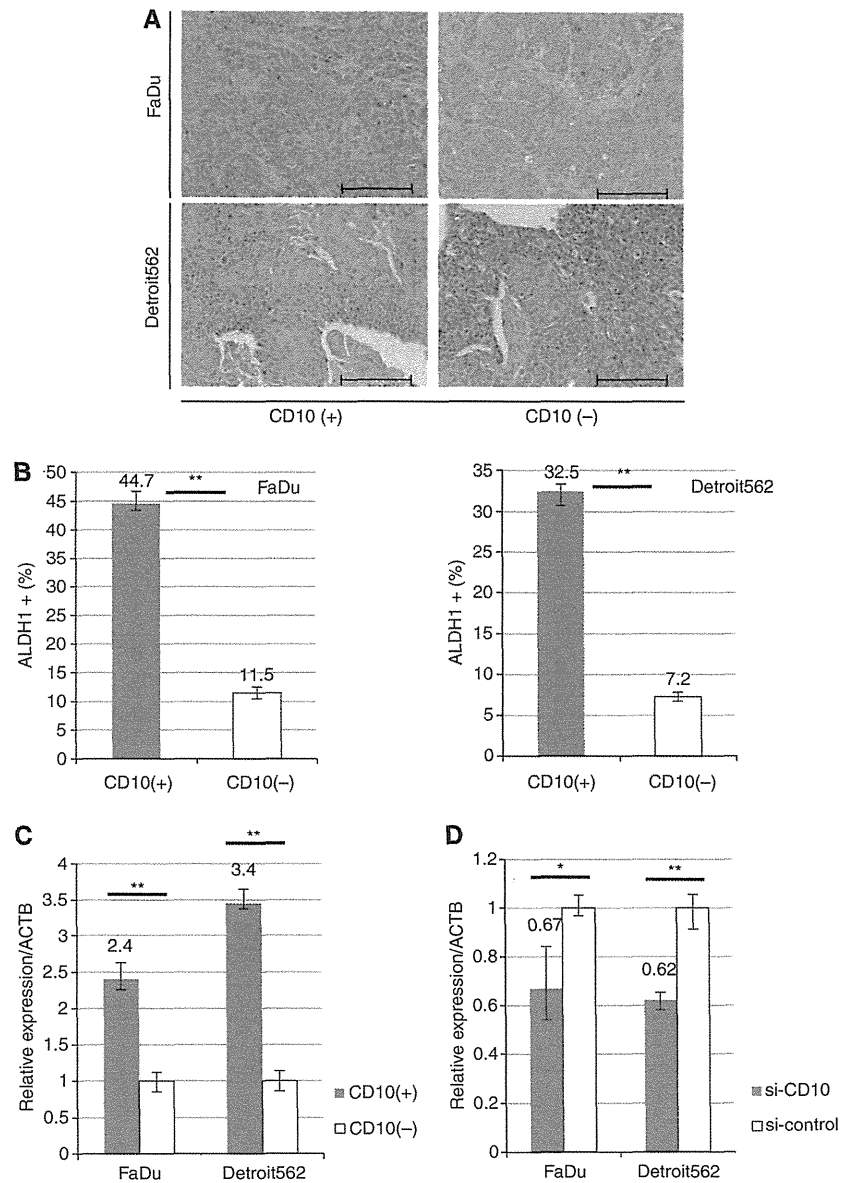
Figure 4. Histology of tumours from CD10(+)/(−) subpopulations and the relationship between CD10 and other stem cell markers. (A) H&E staining of FaDu and Detroit562 xenograft tumours. Scale bar, 100 μM. (B) Expression of ALDH1 in CD10(+)/(−) FaDu and Detroit562 cells was assessed by FACS. Data represent means ± s.e.m.; **$P<0.01$. (C) OCT3/4 expression in CD10(+)/(−) FaDu and Detroit562 cells was assessed by qRT–PCR. (D) OCT3/4 expression in FaDu and Detroit562 following transfection with either si-CD10 or si-control was assessed by qRT–PCR. Gene expression levels are presented as a ratio of the internal control, ACTB ± s.e.m. *$P<0.05$; **$P<0.01$.

metalloendoprotease that cleaves signalling peptides (Roques et al, 1993; Turner & Tanzawa, 1997). It is expressed in a wide range of normal cells, and has been shown to be a cell surface marker of tissue stem cells in the bone marrow (Galy et al, 1998), adipose (Buhring et al, 2007), lung (Sunday et al, 1992) and breast (Stingl et al, 2005). CD10 is also expressed in a series of malignancies originating from the kidney, lung, skin, pancreas, prostate, liver, breast, stomach, cervix and bladder. Several studies have shown an association between CD10 and metastasis (Maguer-Satta et al, 2011). In HNSCC, an involvement of CD10 in tumour differentiation and growth has been reported (Piattelli et al, 2006). This report also showed that expression of CD10 was associated with distant metastases, local recurrences and histological grade in HNSCC patients. Because of this background and our experiments, we hypothesised that CD10 is a marker for refractory HNSCC. Thus, we further examined whether the CD10-positive subpopulation was chemo and/or radio resistant. We found that the CD10-positive subpopulation was more resistant to treatment with cisplatin, fluorouracil or radiation in comparison with the CD10-negative subpopulation.

Several mechanisms, such as efficient DNA repair and expression of transporter pumps, as well as changes in cell cycling are considered to explain such resistance. Among these mechanisms, we focussed on the cell cycle. We analysed cell cycle phase distributions between CD10-positive and CD10-negative subpopulations. We found that the percentage of G0/G1 phase cells was increased in CD10-positive subpopulation when compared with that of the CD10-negative subpopulation. This result indicates that the CD10-positive subpopulation of HNSCC cells was slow-cell cycling or dormant compared with CD10-negative subpopulation.

Recent studies have shown that CSCs are responsible for the therapeutic resistance of cancers (Bao et al, 2006; Li et al, 2008).

−59−

Additionally, CSCs are slow-cycling or in the dormant phase of the cell cycle. For example, CSCs of acute myeloid leukaemia (Guan *et al*, 2003) and chronic myeloid leukaemia (Holyoake *et al*, 1999) survive in the dormant G0 phase of the cell cycle. In the case of solid tumours, liver CSCs were found to be mainly in the G0/G1 phase (Haraguchi *et al*, 2010). Thus, we addressed the relevance of CD10 for the CSC phenotype. We found that the CD10-positive subpopulation formed spheres *in vitro* and tumours *in vivo* more efficiently than the CD10-negative subpopulation. These results indicate that CD10 is closely related to tumourigenicity and self-renewal ability. Thus, it seems likely that CD10 could serve as a marker of CSCs in HNSCC.

Previously, CD44 (Prince *et al*, 2007), CD133 (Chiou *et al*, 2008) and ALDH1 (Chen *et al*, 2009) have been reported as markers of CSCs in HNSCC. However, whether CD44 and ALDH1 serve as true markers remains controversial. For instance, recent studies have shown that decreased rather than increased expression of ALDH1 is linked to poor prognosis (Koukourakis *et al*, 2012), while CD44 is expressed in normal head and neck squamous epithelium at an equivalent level to that detected in HNSCC (Chen *et al*, 2011). As for therapeutic resistance, CD44 expression was downregulated in irradiated cells when compared with that of untreated cells as determined in our cell surface antigen array assay of the HNSCC cell line BICR6. Moreover, the vast majority of FaDu and Detroit562 cells were CD44-positive irrespective of cisplatin or radiation treatment. In the case of CD133, Zhang *et al*, (2010) showed that CD133-positive cells possessed resistance to paclitaxel when compared with CD133-negative cells in oral cancer cell lines, although CD133 expression was barely detectable, even after the treatment, in the cell lines used in our study. Together, these data indicate that neither CD44 nor CD133 have pivotal roles in the therapeutic resistance of these HNSCC cell lines. Although it cannot be dismissed that the relevance of CD44 and CD133 in therapeutic resistance probably depends on the kinds of cells lines and treatments administered. Thus, further study is needed to determine the relationship between CSC-related properties and therapeutic resistant in HNSCC, including investigation into the effect of combination of CD10 and these markers (CD44, CD133, ALDH1). Especially, we consider the combination of CD10 and ALDH1, because we found these interdependent expressions.

Notably, we demonstrated that the CD10-positive subpopulation of HNSCC cells showed CSC-related properties, such as chemo and radio resistance, self-renewal capacity and tumourigenicity. To gain insight into the mechanisms by which CD10 confers CSC-related properties in HNSCC, we examined the expression of *OCT3/4*, which has a critical role in the development and self-renewal of embryonic stem cells (Nichols *et al*, 1998), and is linked to oncogenic processes (Gidekel *et al*, 2003). Chen *et al*, (2010, 2011). have shown that *OCT3/4* is upregulated in HNSCC CSCs, defined by ALDH1 positive cells, and in spheroid forming HNSCC cells. We found that *OCT3/4* expression was higher in CD10-positive cells than in CD10-negative cells, but that it was decreased following knockdown of CD10. These results indicate that increased CD10 is linked to *OCT3/4* expression. Further studies are required to address the functional relevance of CD10 to *OCT3/4* in HNSCC.

In conclusion, we have established that CD10 is associated with chemo and radio resistance, and that it confers CSC-related properties in HNSCC, probably through forced overexpression of *OCT3/4*. Together these findings suggest that CD10 may serve as a target molecule in the treatment of refractory HNSCC.

REFERENCES

Argiris A, Karamouzis MV, Raben D, Ferris RL (2008) Head and neck cancer. *Lancet* 371(9625): 1695–1709.

Bao S, Wu Q, McLendon RE, Hao Y, Shi Q, Hjelmeland AB, Dewhirst MW, Bigner DD, Rich JN (2006) Glioma stem cells promote radioresistance by preferential activation of the DNA damage response. *Nature* 444(7120): 756–760.

Barr MP, Gray SG, Hoffmann AC, Hilger RA, Thomale J, O'Flaherty JD, Fennell DA, Richard D, O'Leary JJ, O'Byrne KJ (2013) Generation and characterisation of cisplatin-resistant non-small cell lung cancer cell lines displaying a stem-like signature. *PloS one* 8(1): e54193.

Buhring HJ, Battula VL, Treml S, Schewe B, Kanz L, Vogel W (2007) Novel markers for the prospective isolation of human MSC. *Ann NY Acad Sci* 1106: 262–271.

Chen C, Wei Y, Hummel M, Hoffmann TK, Gross M, Kaufmann AM, Albers AE (2011) Evidence for epithelial-mesenchymal transition in cancer stem cells of head and neck squamous cell carcinoma. *PloS one* 6(1): e16466.

Chen YC, Chang CJ, Hsu HS, Chen YW, Tai LK, Tseng LM, Chiou GY, Chang SC, Kao SY, Chiou SH, Lo WL (2010) Inhibition of tumorigenicity and enhancement of radiochemosensitivity in head and neck squamous cell cancer-derived ALDH1-positive cells by knockdown of Bmi-1. *Oral Oncol* 46(3): 158–165.

Chen YC, Chen YW, Hsu HS, Tseng LM, Huang PI, Lu KH, Chen DT, Tai LK, Yung MC, Chang SC, Ku HH, Chiou SH, Lo WL (2009) Aldehyde dehydrogenase 1 is a putative marker for cancer stem cells in head and neck squamous cancer. *Biochem Biophys Res Commun* 385(3): 307–313.

Chiou SH, Yu CC, Huang CY, Lin SC, Liu CJ, Tsai TH, Chou SH, Chien CS, Ku HH, Lo JF (2008) Positive correlations of Oct-4 and Nanog in oral cancer stem-like cells and high-grade oral squamous cell carcinoma. *Clin Cancer Res* 14(13): 4085–4095.

Galy A, Morel F, Hill B, Chen BP (1998) Hematopoietic progenitor cells of lymphocytes and dendritic cells. *J Immunother* 21(2): 132–141.

Gidekel S, Pizov G, Bergman Y, Pikarsky E (2003) Oct-3/4 is a dose-dependent oncogenic fate determinant. *Cancer Cell* 4(5): 361–370.

Guan Y, Gerhard B, Hogge DE (2003) Detection, isolation, and stimulation of quiescent primitive leukemic progenitor cells from patients with acute myeloid leukemia (AML). *Blood* 101(8): 3142–3149.

Haraguchi N, Ishii H, Mimori K, Tanaka F, Ohkuma M, Kim HM, Akita H, Takiuchi D, Hatano H, Nagano H, Barnard GF, Doki Y, Mori M (2010) CD13 is a therapeutic target in human liver cancer stem cells. *J Clin Invest* 120(9): 3326–3339.

Holyoake T, Jiang X, Eaves C, Eaves A (1999) Isolation of a highly quiescent subpopulation of primitive leukemic cells in chronic myeloid leukemia. *Blood* 94(6): 2056–2064.

Kish J, Drelichman A, Jacobs J, Hoschner J, Kinzie J, Loh J, Weaver A, Al-Sarraf M (1982) Clinical trial of cisplatin and 5-FU infusion as initial treatment for advanced squamous cell carcinoma of the head and neck. *Cancer Treat Rep* 66(3): 471–474.

Koukourakis MI, Giatromanolaki A, Tsakmaki V, Danielidis V, Sivridis E (2012) Cancer stem cell phenotype relates to radio-chemotherapy outcome in locally advanced squamous cell head-neck cancer. *Br J Cancer* 106(5): 846–853.

Li X, Lewis MT, Huang J, Gutierrez C, Osborne CK, Wu MF, Hilsenbeck SG, Pavlick A, Zhang X, Chamness GC, Wong H, Rosen J, Chang JC (2008) Intrinsic resistance of tumorigenic breast cancer cells to chemotherapy. *J Natl Cancer Inst* 100(9): 672–679.

Lo WL, Kao SY, Chi LY, Wong YK, Chang RC (2003) Outcomes of oral squamous cell carcinoma in Taiwan after surgical therapy: factors affecting survival. *J Oral Maxillofac Surg* 61(7): 751–758.

Maguer-Satta V, Besancon R, Bachelard-Cascales E (2011) Concise review: neutral endopeptidase (CD10): a multifaceted environment actor in stem cells, physiological mechanisms, and cancer. *Stem Cells* **29**(3): 389–396.

Nichols J, Zevnik B, Anastassiadis K, Niwa H, Klewe-Nebenius D, Chambers I, Scholer H, Smith A (1998) Formation of pluripotent stem cells in the mammalian embryo depends on the POU transcription factor Oct4. *Cell* **95**(3): 379–391.

Piattelli A, Fioroni M, Iezzi G, Perrotti V, Stellini E, Piattelli M, Rubini C (2006) CD10 expression in stromal cells of oral cavity squamous cell carcinoma: a clinic and pathologic correlation. *Oral Dis* **12**(3): 301–304.

Prince ME, Sivanandan R, Kaczorowski A, Wolf GT, Kaplan MJ, Dalerba P, Weissman IL, Clarke MF, Ailles LE (2007) Identification of a subpopulation of cells with cancer stem cell properties in head and neck squamous cell carcinoma. *Proc Natl Acad Sci USA* **104**(3): 973–978.

Roques BP, Noble F, Dauge V, Fournie-Zaluski MC, Beaumont A (1993) Neutral endopeptidase 24.11: structure, inhibition, and experimental and clinical pharmacology. *Pharmacol Rev* **45**(1): 87–146.

Sinclair WK (1968) Cyclic X-ray responses in mammalian cells *in vitro*. *Radiation research* **33**: 620–643.

Stingl J, Raouf A, Emerman JT, Eaves CJ (2005) Epithelial progenitors in the normal human mammary gland. *J Mammary Gland Biol Neoplasia* **10**(1): 49–59.

Sunday ME, Hua J, Torday JS, Reyes B, Shipp MA (1992) CD10/neutral endopeptidase 24.11 in developing human fetal lung. Patterns of expression and modulation of peptide-mediated proliferation. *J Clin Invest* **90**(6): 2517–2525.

Turner AJ, Tanzawa K (1997) Mammalian membrane metallopeptidases: NEP, ECE, KELL, and PEX. *FASEB J* **11**(5): 355–364.

Zhang Q, Shi S, Yen Y, Brown J, Ta JQ, Le AD (2010) A subpopulation of CD133(+) cancer stem-like cells characterized in human oral squamous cell carcinoma confer resistance to chemotherapy. *Cancer Lett* **289**(2): 151–160.

Supplementary Information accompanies this paper on British Journal of Cancer website (http://www.nature.com/bjc)

MicroRNA-1246 expression associated with CCNG2-mediated chemoresistance and stemness in pancreatic cancer

S Hasegawa[1,2], H Eguchi[1], H Nagano[1], M Konno[2], Y Tomimaru[1], H Wada[1], N Hama[1], K Kawamoto[1], S Kobayashi[1], N Nishida[2], J Koseki[3], T Nishimura[4], N Gotoh[4], S Ohno[5], N Yabuta[5], H Nojima[5], M Mori[1], Y Doki[1] and H Ishii[*,2,3]

[1]Department of Gastroenterological Surgery, Osaka University, Graduate School of Medicine, 2-2, Yamadaoka, Suita, Osaka 565-0871, Japan; [2]Department of Frontier Science for Cancer and Chemotherapy, Osaka University, Graduate School of Medicine, 2-2, Yamadaoka, Suita, Osaka 565-0871, Japan; [3]Department of Cancer Profiling Discovery, Osaka University, Graduate School of Medicine, 2-2, Yamadaoka, Suita, Osaka 565-0871, Japan; [4]Division of Molecular Therapy, Molecular Targets Laboratory, Institute of Medical Science, University of Tokyo, 4-6-1, Shirokanedai, Minato-ku, Tokyo 108-8639, Japan and [5]Department of Molecular Genetics, Research Institute for Microbial Diseases, Osaka University, 3-1, Yamadaoka, Suita, Osaka 565-0871, Japan

Background: Pancreatic cancer has a poor prognosis because of its high refractoriness to chemotherapy and tumour recurrence, and these properties have been attributed to cancer stem cells (CSCs). MicroRNA (miRNA) regulates various molecular mechanisms of cancer progression associated with CSCs. This study aimed to identify the candidate miRNA and to characterise the clinical significance.

Methods: We established gemcitabine-resistant Panc1 cells, and induced CSC-like properties through sphere formation. Candidate miRNAs were selected through microarray analysis. The overexpression and knockdown experiments were performed by evaluating the in vitro cell growth and in vivo tumourigenicity. The expression was studied in 24 pancreatic cancer samples after laser captured microdissection and by immunohistochemical staining.

Results: The in vitro drug sensitivity of pancreatic cancer cells was altered according to the miR-1246 expression via CCNG2. In vivo, we found that miR-1246 could increase tumour-initiating potential and induced drug resistance. A high expression level of miR-1246 was correlated with a worse prognosis and CCNG2 expression was significantly lower in those patients.

Conclusions: miR-1246 expression was associated with chemoresistance and CSC-like properties via CCNG2, and could predict worse prognosis in pancreatic cancer patients.

Pancreatic cancer has the worst prognosis of any major malignancy and is the fourth most common cause of cancer death each year in the United States. Even if it is diagnosed at an operable stage and curative resection is achieved, there is still a high incidence of recurrence (Hoyert et al, 2006). Although gemcitabine (GEM)-based chemotherapy has formed the core of multimodal therapy for pancreatic cancer (Oettle et al, 2007), it is rarely curative and only modestly effective against tumour recurrence. Cancer stem cells (CSCs) have been implicated in the clinical refractoriness, metastasis, and tumour recurrence of various types of cancer, including pancreatic cancer (Hermann et al, 2007; Li et al, 2007). The molecular mechanisms that link chemoresistance with CSCs remain unclear. Clarifying these mechanisms could improve prognosis of patients with pancreatic cancer.

*Correspondence: Professor H Ishii; E-mail: hishii@gesurg.med.osaka-u.ac.jp

The miRNAs are endogenous, 18–25-bp, single-stranded, non-coding modulators of the post-transcriptional process (Bartel, 2009). In the present study, we focused on miRNAs of GEM-resistant pancreatic cancer cell lines and CSC-like cell populations using sphere formation assays (Pastrana et al, 2011); pancreatic CSCs could be enriched as spheroid cells (Hermann et al, 2007). We performed comprehensive expression profiling of miRNAs in order to indentify the candidate miRNA and determine its clinical significance.

MATERIALS AND METHODS

Vector constructs and lentiviral production. The lentiviral pLenti-III-miR-1246 vector and its empty pLenti-III vector (Applied Biological Materials Inc., Richmond, Canada) were co-transfected with pCAG-HIVgp and pCMV-VSV-G-RSV-Rev into 293Ta cells (Gene Copoeia Inc., Rockville, MD, USA). Panc1 cells were infected with lentivirus and selected using $1 \mu g \, ml^{-1}$ puromycin for 4 weeks, to establish stable miR-1246 (Panc1-P-l-OE) and control (Panc1-P-l-C) transfectants. The *CCNG2* lacking

miR1246 target sites in 3′UTR were transfected into the Panc1-P-l-OE cells using FuGENE 6 Reagent (Promega, Madison, WI, USA).

Ethics statement on animals. All animal work was performed according to Animal Experiments Committee, Osaka University (the approval number, 24-122-011).

Animal experiments. Four different numbers of Panc1 cells, 1×10^2, 1×10^3, 1×10^4, and 1×10^5, were injected subcutaneously in 4- to 6-week-old female non-obese mice with diabetes/severe combined immunodeficiency (CLEA Japan, Tokyo, Japan). The mice were administered GEM intraperitoneally three times on days 35, 42, and 49 using the once-a-week protocol as to closely replicate clinical use. Mice were given $125 \, mg \, kg^{-1}$ GEM, or phosphate-buffered saline as control (Lonardo et al, 2011). The tumour volume was calculated as: (longest diameter) × (shortest diameter)^2 × 0.5. The therapy was initiated when the tumour volumes were 60–100 mm^3. The tumours were resected on day 53 after the cell injection. Total RNA was extracted from tumours. Immunohistochemistry was performed using polyclonal goat anti-human cyclinG2 antibody (Santa Cruz Biotechnology Inc., Santa Cruz, CA, USA).
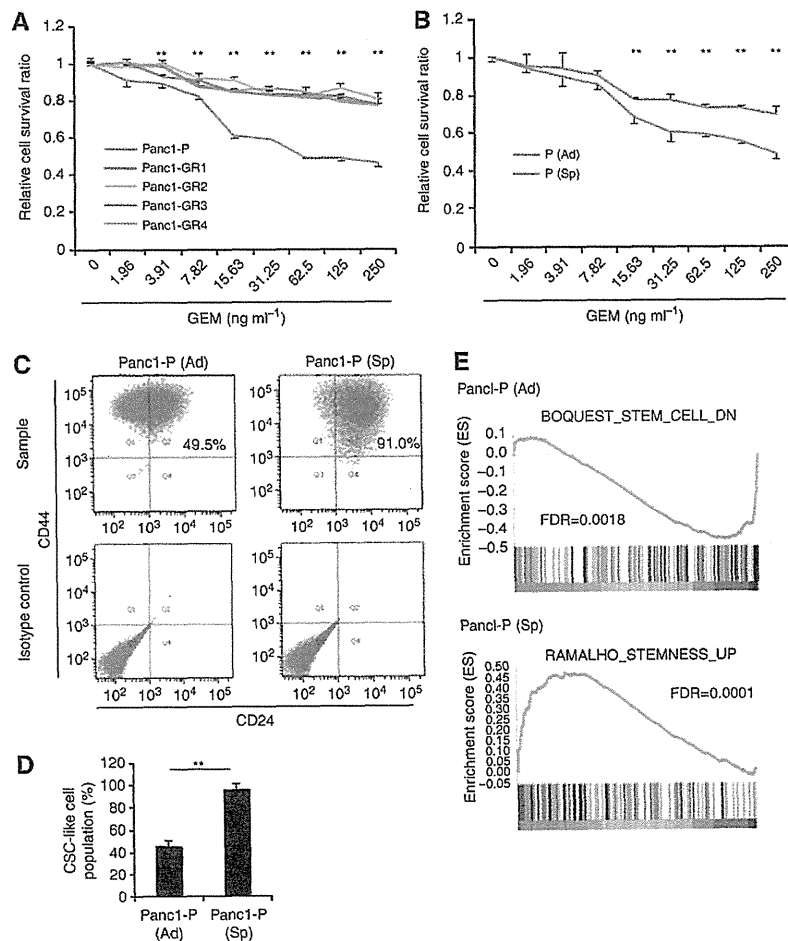

Figure 1. Features of gemcitabine (GEM)-resistant pancreatic cancer cells (Panc1-GRs) and Panc1 parental CSC-like spheroid cells (Panc1-P (Sp)). (A) Growth-inhibitory effects of GEM on Panc1 parental (Panc1-P) cells and Panc1-GR (GR1, GR2, GR3, and GR4) cells were assessed by MTT assay. (B) Growth-inhibitory effects of GEM on normal adherent condition Panc1-P (Ad) and Panc1-P (Sp) cells were assessed by MTT assay. (C) The representative data of flow cytometry showed the CSC-like cell population of Panc1-P in Panc1-P (Ad) cells (left panel) and Panc1-P (Sp) cells (right panel). (D) The percentages of the CSC-like cell populations were shown in Pan1-P (Ad) and -P (Sp) cells. This assay was performed three times. (E) Gene set enrichment analysis (GSEA) of Panc1-P (Sp) cells compared with Panc1-P (Ad) cells was performed. GSEA-extracted representative gene sets enriched in those cells are shown. Data represent mean ± s.d. of more than three experiments; **$P < 0.01$.

Ethics statement on clinical samples. The use of resected samples was approved by the Human Ethics Review Committee of the Graduate School of Medicine, Osaka University (approval number 08226). Written informed consent was obtained from all patients included in the study.

Study on primary tumour samples. Between March 2007 and December 2010, 24 consecutive patients with pancreatic cancer were treated by histologically curative resection (R0) at Osaka University Hospital, and no preoperative therapy was given (Supplementary Table 3). Among 24 patients, 12 patients received adjuvant GEM chemotherapy. Immunohistochemical staining protocol is shown in the Supplementary Materials and Methods. To separate epithelial and mesenchymal parts, laser captured microdissection (LCM; LMD7000, Leica Microsystems GmbH, Wetzlar, Germany) was performed as 8-μm-thick sections from formalin-fixed paraffin-embedded (FFPE) samples. Total RNA was extracted using RNeasy FFPE Kit (Qiagen, Tokyo, Japan). The relative quantification of miRNA was studied by qRT-PCR using comparative CT method $(2^{-\Delta CT})$. Data were normalised using endogenous RNU48 control.

Statistical analysis. The clinicopathological parameters were compared using the Fisher's exact test, and the continuous variables were compared using the Student's t-test. The survival curves were computed using the Kaplan–Meier method. Statistical analysis was performed using JMP software version 10.0.2 (SAS Institute Inc., Cary, NC, USA).

RESULTS

Establishment of GEM-resistant pancreatic cancer cell clones. We established four independent GEM-resistant clones of Panc1 cells. Compared with the Panc1-P cells, the Panc1-GR cells were significantly more resistant to GEM (Figure 1A) and showed significantly more drug resistance to 5-FU at three densities (Supplementary Figure 1A). Several studies have recently reported that representative surface markers, such as CD44 + CD24 +, were useful to enrich the CSC-like cells from others in pancreatic cancer cell lines (Hermann *et al*, 2007; Li *et al*, 2007). Flow cytometry analysis of the CSC population in Panc1-GRs revealed that the CD44 + CD24 + population was slightly increased (Figure 1B and Supplementary Figure 1B).

Establishment of pancreatic CSC-like chemoresistant cells. The sphere formation and growth assays revealed that Panc1-P (Sp) was significantly resistant to GEM and 5-FU compared with Panc1-P (Figure 1B and Supplementary Figure 1D). Note that Panc1-P (Sp) cells were chemoresistant to GEM and 5-FU, although not exposed to agents. Flow cytometry analysis revealed
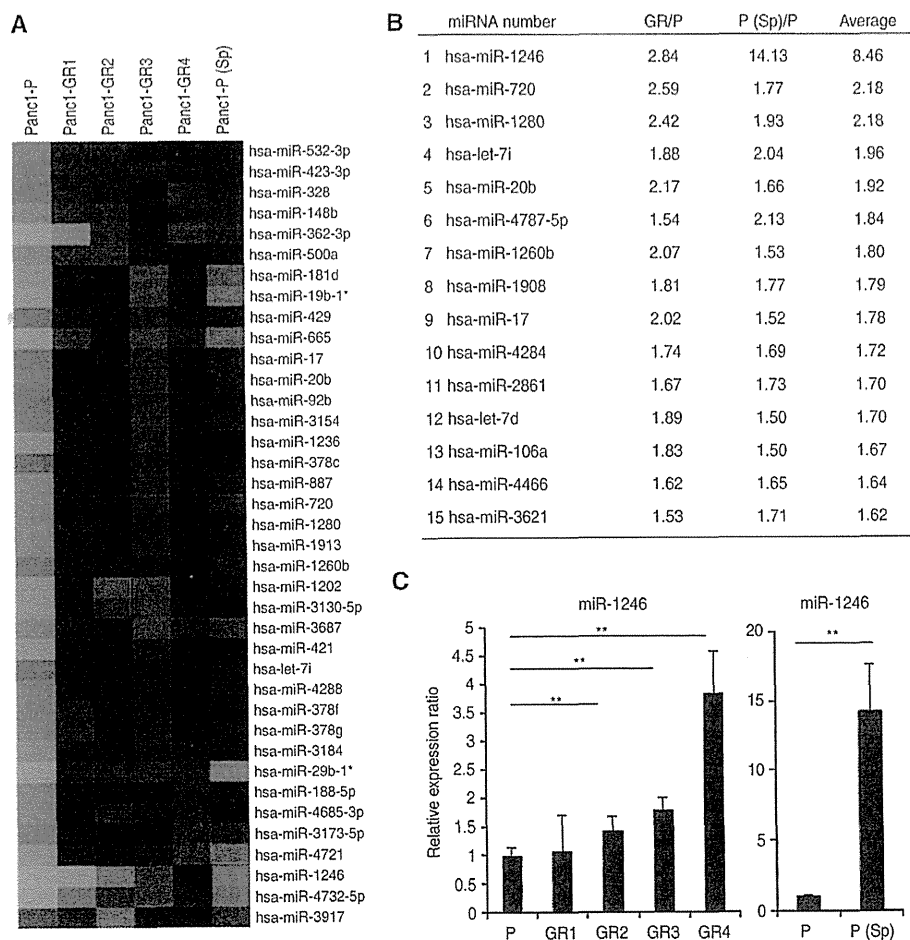
A

	miRNA number	GR/P	P (Sp)/P	Average
1	hsa-miR-1246	2.84	14.13	8.46
2	hsa-miR-720	2.59	1.77	2.18
3	hsa-miR-1280	2.42	1.93	2.18
4	hsa-let-7i	1.88	2.04	1.96
5	hsa-miR-20b	2.17	1.66	1.92
6	hsa-miR-4787-5p	1.54	2.13	1.84
7	hsa-miR-1260b	2.07	1.53	1.80
8	hsa-miR-1908	1.81	1.77	1.79
9	hsa-miR-17	2.02	1.52	1.78
10	hsa-miR-4284	1.74	1.69	1.72
11	hsa-miR-2861	1.67	1.73	1.70
12	hsa-let-7d	1.89	1.50	1.70
13	hsa-miR-106a	1.83	1.50	1.67
14	hsa-miR-4466	1.62	1.65	1.64
15	hsa-miR-3621	1.53	1.71	1.62

Figure 2. miRNA microarray analysis and the ranking of candidate miRNAs. (A) The heat map revealed the miRNAs whose expression levels were altered > 1.5-fold relative to Panc1-P both in Panc1-GRs and -P (Sp) cells. *non-functional miRNA. (B) The list showed the ranking of candidate miRNAs according to the ratio of the change in expression level. From the above 38 miRNAs (A), 15 miRNAs were selected. (C) Real-time qRT–PCR showed the expression of miR-1246 in Panc1-P, -GRs, and -P (Sp) cells. Data represent mean ± s.d. of more than three experiments; **$P<0.01$.

—64—

that the CD24 + CD44 + population nearly doubled due to sphere formation (Figure 1C and D).

Gene sets enriched in spheroid cells and adherent cells. Gene set enrichment analysis (GSEA) was performed between the coding gene expression profiles of the spheroid parental Panc1 (Panc1-P (Sp)) cells and those of the adherent parental cells (Panc1-P). The GSEA in spheroid cells revealed upregulation of stem cell pathway

and downregulation of adherent pathway (Figure 1E and Supplementary Figure 2A and B).

Outstanding expression of miR-1246 revealed by miRNA microarray analysis. To identify the candidate miRNAs related to chemoresistance and cancer stemness, we performed miRNA microarray studies. The data showed that, among the 1719 miRNAs, the miRNA expression levels of 92 in the Panc1-GR
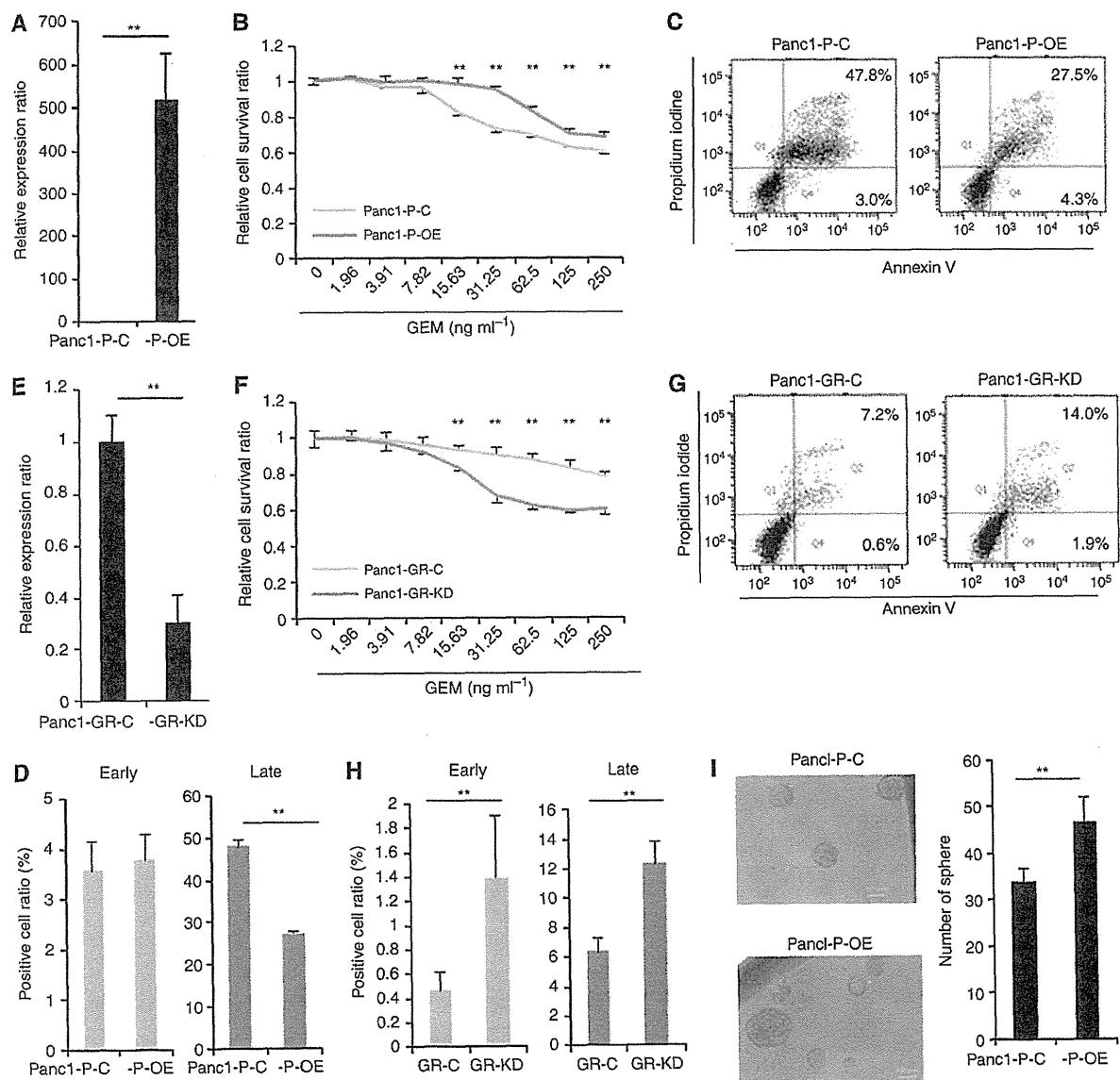

Figure 3. Association of miR-1246 expression with the resistance to GEM and sphere-forming ability. (A) Real-time qRT–PCR showed the expression level of miR-1246 in Panc1-P cells transfected with pre-miR-1246 (Panc1-P-OE) and transfected with the negative control (Panc1-P-C). (B) MTT assay demonstrated relative cell survival ratio of Panc1-P-C and Panc1-P-OE cells to GEM, respectively. (C) The representative data of Annexin V assay showed the distribution of the early and late apoptotic cells in the Panc1-P-C and Panc1-P-OE cells after GEM exposure for 72 h. (D) The percentages of early and late apoptotic cells in the Panc1-P-C and Panc1-P-OE cells after GEM exposure for 72 h. This assay was performed three times. (E) Real-time qRT–PCR showed the expression level of miR-1246 in Panc1-GR cells transfected with anti-miR-1246 (Panc1-GR-KD) and transfected with negative control (Panc1-GR-C). (F) MTT assay demonstrated relative cell survival ratio of Panc1-GR-C and Panc1-GR-KD to GEM. (G) The representative data of Annexin V assay showed the distribution of the early and late apoptotic cells in Panc1-GR-C and Panc1-GR-KD cells after GEM exposure for 72 h. (H) The percentages of early and late apoptotic cells in Panc1-GR-C and Panc1-GR-KD cells after GEM exposure for 72 h. This assay was performed three times. (I) Sphere formation assay was performed in Panc1-P-C and Panc1-P-OE cells. The representative image of spheres (left) and the number of spheres (right) were shown. Bar = 100 μm. Data represent mean ± s.d. of three experiments; **P < 0.01.

cells (Supplementary Table 1) and 216 in the Panc1-P (Sp) cells (Supplementary Table 2) were altered by an average of >1.5-fold relative to the parental levels. The heat map showed 38 common miRNAs, which included 37 miRNAs (>1.5-fold) and 1 miRNA (<0.66-fold) of the parental levels (Figure 2A). By excluding 23 miRNAs that showed undetectable or extremely low expression and non-functional miRNAs, we found 15 candidate miRNAs were expressed strongly in both Panc1-GRs and Panc1-P (Sp) cells (Figure 2B). miR-1246 showed the highest alteration (8.46 average fold change: 14.13-fold increase in the Panc1-P (Sp) and 2.84-fold increase in the Panc1-GR). The fold change of the miR-1246 expression level was outstanding in Panc1-P (Sp) cells. The real-time qRT–PCR confirmed the miR-1246 upregulation in Panc1-GRs and -P (Sp) cells (Figure 2C). We then assessed miR-1246 for further analysis.

Association of miR-1246 expression with the resistance to GEM and sphere-forming ability. To evaluate the effect of miR-1246 on the response to GEM in Panc1 cells, pre- or anti-miR-1246 was

introduced into Panc1-P/-GR4. Real-time qRT–PCR confirmed that the transfection with pre-miR-1246 resulted in the marked overexpression of mature miR-1246 (Panc1-P-OE; Figure 3A). The proliferation rate of the Panc1-P-OE cells was slightly increased compared with control Panc1-P-C. The MTT assay demonstrated that transfection of pre-miR-1246 into Panc1-P resulted in resistance to GEM (Figure 3B). In contrast, anti-miR-1246 transfection into Panc1-GR4, whose endogenous levels of miR-1246 was 3.5-fold higher than that of Panc1-P (Figure 2C), resulted in sufficient inhibition of miR-1246 by qRT–PCR (Panc1-GR-KD; Figure 3E). MTT assay demonstrated a significant reduction of chemoresistance to GEM in the Panc1-GR-KD cells (Figure 3F). The proliferation rate of the Panc1-GR-KD cells was not changed compared with control Panc1-GR-C. These results indicated that miR-1246 induced GEM-resistance in Panc1 cells. We assessed the sphere-forming ability. The proliferation ratio of spheres in Panc1-P-OE was significantly higher than that in Panc1-P-C (Supplementary Figure 1C). Panc1-P-OE spheres increased compared to Panc1-P-C (Figure 3I). We confirm the results with
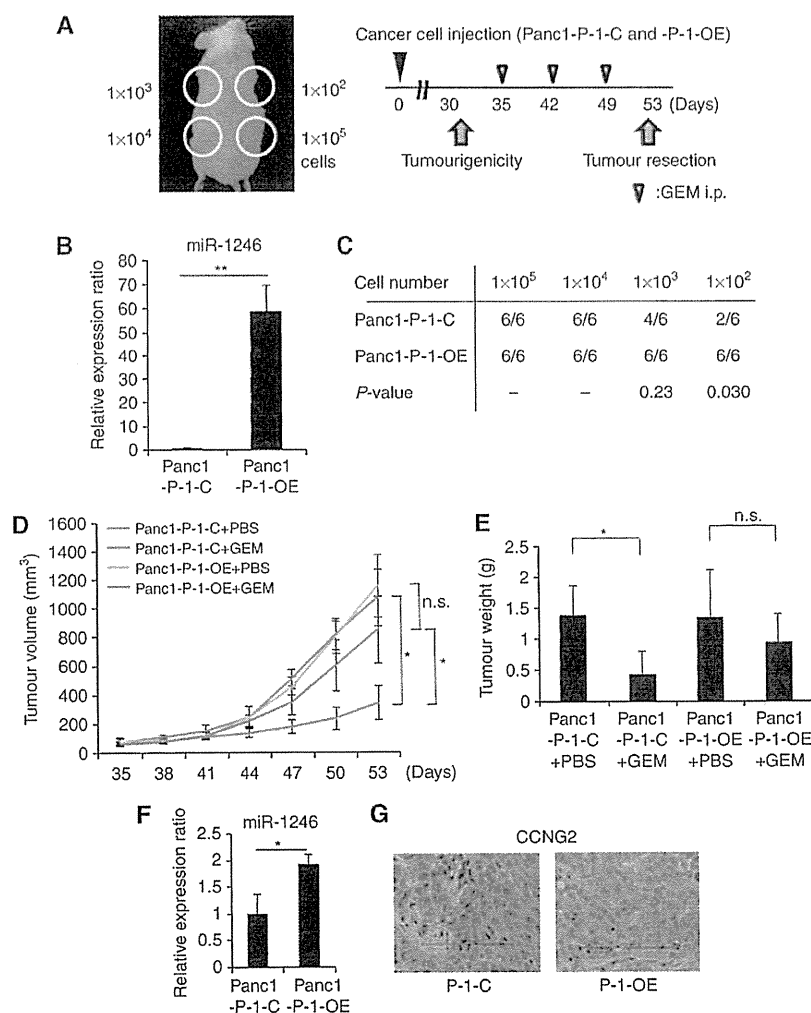

Figure 4. The function of miR-1246 in tumourigenicity and GEM-resistance *in vivo*. (A) The experimental design was shown. (B) Real-time qRT–PCR showed the expression level of miR-1246 in miR-1246 continuously expressing Panc1 (Panc1-P-I-OE) and control Panc1 (Panc1-P-I-C) cells. (C) The tumourigenic ability was evaluated on day 30 after Panc1 cell injection in the Panc1-P-I-C and Panc1-P-I-OE groups. (D) The therapy was initiated when the tumour volumes (1 × 10⁵ cells injected) were between 60 and 100 mm³. (E) The weights of tumours were measured at day 53 after resection. (F) Real-time qRT–PCR showed the expression level of miR-1246 in the tumours of Panc1-P-I-OE and Panc1-P-I-C cell-injected groups. (G) Immunohistochemistry of the tumour specimens showed CCNG2 expression in the tumours of Panc1-P-I-OE and Panc1-P-I-C cell-injected groups. Bar = 100 μm. Data represent mean ± s.d. of three experiments; $*P<0.05$; $**P<0.01$.

another pancreatic cancer cell line, MiaPaCa2 with endogenous miR-1246 decreased (40% of Panc1; Supplementary Figure 4A). The pre-miR-1246 transfection resulted in replenishment of miR-1246 (Supplementary Figure 4C). The MTT assay demonstrated that miR-1246 anti-sensitised MiaPaCa2 to GEM treatment (Supplementary Figure 4E). Although CSC-like cell population was relatively rare (Supplementary Figure 4B), the miR-1246 OE (Sp) enriched by sphere assay revealed that the proliferation rate was higher than control cells (Supplementary Figure 4D). The miR-1246 OE sphere increased significantly compared to control (Supplementary Figure 4F).

miR-1246 induced tumourigenicity and refractoriness to GEM. Although pre-miR-1246 expression continued for a week, it decreased

gradually (Supplementary Figure 3A; the data of anti-miR-1246 in Supplementary Figure 3B). To assess miR-1246 functions relating to tumourigenicity and refractoriness to GEM *in vivo* (Figure 4A), we established Panc1 (Panc1-P-l-OE) cells that overexpressed miR-1246 continuously in high level (Supplementary Figure 3C). We confirmed that the expression level of miR-1246 in Panc1-P-l-OE was ∼50-fold higher than that in Panc1-l-C (Figure 4B). The tumourigenicity of Panc1-P-l-OE was significantly increased compared with Panc1-P-l-C (at 1×10^2 cell injection; Figure 4C). The tumour volume and weight of Panc1-P-l-C, but not Panc1-P-l-OE, was significantly inhibited by GEM treatment compared with controls at day 53 (Figure 4D and E). The miR-1246 expression in the Panc1-P-l-OE tumours was significantly two times higher than the expression in Panc1-P-l-C at day 53 (Figure 4F).
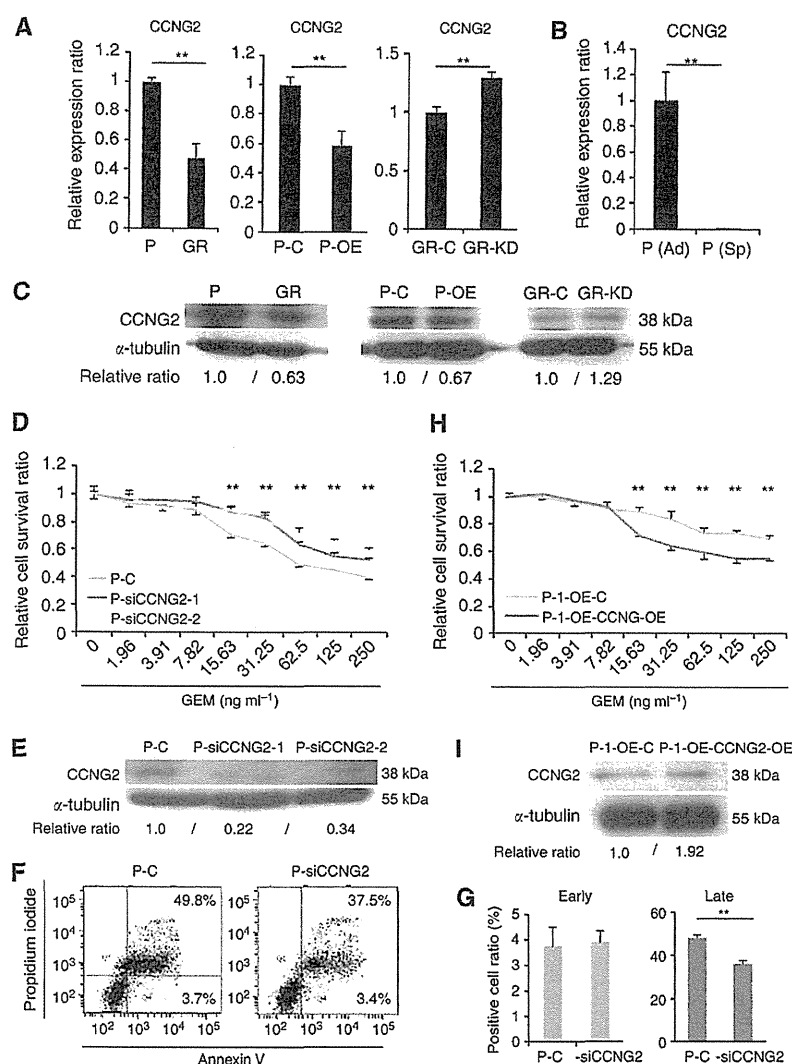

Figure 5. The *CCNG2* function as a target of miR-1246 in Panc1 cells. (A–C) Real-time qRT–PCR and western blotting demonstrated *CCNG2* expression level in Panc1-P and Panc1-GR cells, Panc1-P-C and Panc1-P-OE cells, Panc1-GR-C and Panc1-GR-KD cells, and Panc1-P (Ad) and Panc1-P (Sp) cells. (D) MTT assay demonstrated the relative cell survival ratio of Panc1-P cells transfected with siCCNG2 (Panc1-P-siCCNG2-1, -2) and transfected with negative control (Panc1-P-C). (E) The protein level of *CCNG2* in Panc1-P and GR cells, Panc1-P-C and Panc1-P-OE cells, and Panc1-GR-C and Panc1-GR-KD cells in western blotting. (F) The representative data of Annexin V assay showed the distribution of the early and late apoptotic cells in Panc1-P-C and Panc1-P-siCCNG2 after GEM exposure for 72 h. (G) The percentages of early and late apoptotic cells in Panc1-P-C and Panc1-P-siCCNG2 after GEM exposure for 72 h. This assay was performed three times. (H) MTT assay demonstrated relative cell survival ratio of Panc1-P-l-OE cells transfected with ectopic *CCNG2* (Panc1-P-l-OE-CCNG2-OE) and transfected with control vector (Panc1-P-l-OE-C) to GEM. (I) Western blotting demonstrated *CCNG2* expression level in Panc1-P-l-OE-CCNG2-OE and Panc1-P-l-OE-C. Data represent mean ± s.d. of three experiments; **$P < 0.01$.

miR-1246 inhibits response to GEM by targeting CCNG2. Few studies have reported miR-1246 expression in gastrointestinal cancers, and little is known about the function. As putative miR-1246 targets, the TargetScan (http://www.targetscan.org/) predicted 178 genes. Among them, *CCNG2*, a family of cyclins that is homologous to CCNG1 (Bates *et al*, 1996) and is also known as a tumour suppressor, was selected for further analysis. Western blotting and qRT–PCR showed that *CCNG2* expression was lower in Panc1-GR cells than in Panc1-P cells (Figure 5A and C). Western blotting and qRT–PCR confirmed that pre-miR-1246 transfection decreased *CCNG2* expression, whereas anti-miR-1246 increased it (Figure 5A and C), suggesting that *CCNG2* was one of the target genes of miR-1246. *CCNG2* expression was significantly lower in Panc1-P (Sp) than in control (Figure 5B). We are interested in a role of *CCNG2* in the resistance to GEM. To this end, we performed knockdown of *CCNG2* by siRNA. Western blotting confirmed the knockdown (Figure 5E). The MTT assay demonstrated that transfection of siCCNG2 elicited the resistance of Panc1-P to GEM (Figure 5D). Given reportedly *CCNG2* regulated cell growth and induced apoptosis (Kim *et al*, 2004), we studied the involvement of apoptosis in present case. In Panc1-P, pre-miR-1246 significantly reduced the number of late apoptotic cells (Figure 3C and D). Similarly, pre-miR-1246 significantly reduced the early and late apoptosis in MiaPaCa2 cells

(Supplementary Figure 4G and H). In contrast, the anti-miR-1246 increased the number of early and late apoptotic cells significantly in Panc1-GR (Figure 3G and H). Also, siCCNG2 significantly reduced late apoptosis (Figure 5F and G). These data suggested that miR-1246 regulated chemoresistance via *CCNG2* expression that was involved in apoptosis. Furthermore, in order to study whether the ectopic *CCNG2* expression can rescue the miR-1246-driven GEM-resistance, we transfected *CCNG2* vector (lacking miR-1246 target sites) into Panc1-P-l-OE cells. The MTT assay demonstrated that ectopic *CCNG2* significantly reduced chemoresistance to GEM in the Panc1-P-l-OE cells (Figure 5H); the elevation of *CCNG2* expression was confirmed with western blotting (Figure 5I).

As for the *in vivo* experiment mentioned above, qRT–PCR and immunohistochemistry demonstrated that the *CCNG2* expression was decreased in both the mRNA (data not shown) and protein levels (Figure 4G) in the Panc1-P-l-OE tumours at day 53. This result supported the conclusion that *CCNG2* was one of the target genes for miR-1246.

miR-1246 and CCNG2 expression in primary pancreatic cancer samples. To study the clinical significance, we performed LCM to collect cancer sections from tumour tissues, qRT–PCR, and immunohistochemistry in 24 patients who underwent R0 resection
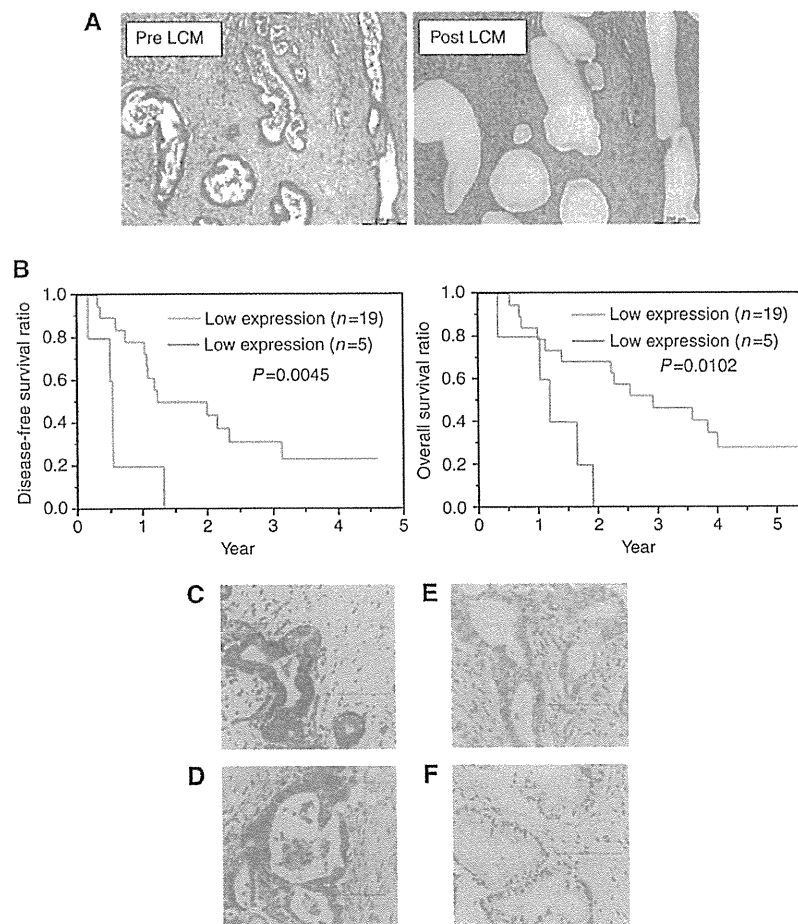

Figure 6. miR-1246 and *CCNG2* expression in primary pancreatic cancer samples. (A) The representative image of pre/post (left/right) laser captured microdissection (LCM). Bar = 200 μm. (B) Relationships between miR-1246 expression and disease-free survival, or overall survival. (C–F) Immunohistochemical staining of *CCNG2* in 24 primary tumours. The *CCNG2*-positive cases show the diffuse (C) or spotted (D) nuclear patterns; *CCNG2*-negative ones depict cytoplasmic pattern (E; not stained in the nucleus) or the negative pattern (F; not stained in the nucleus or cytoplasm).

Table 1. The primary pancreatic cancer patients in the present study

	miR-1246 expression		
	Low (n = 19)	High (n = 5)	P-value
Age (<65:⩾65)	7:12	0:5	0.14
Sex (male:female)	12:7	2:3	0.33
Histopathological type (well or mod:poor)	17:2	5:0	0.62
Tumour size (mm)	24.4 ± 14.4	24.6 ± 9.5	0.48
Tumour location (head:body or tail)	8:11	5:0	0.030
Pathological depth of invasion depth pT (T1 or T2:T3)	6:13	0:5	0.20
Pathological lymph node metastasis pN (negative:positive)	12:7	1:4	0.14
Pathological stage (IA or IB or IIA:IIB or IV)	12:7	1:4	0.14
Adjuvant therapy (−/+)	9:10	2:3	0.59
CCNG2 expression (negative:positive)	5:14	4:1	0.047

Abbreviations: mod = moderately differentiated; poor = poorly differentiated; well = well differentiated.

(Figure 6A). The expression level of miR-1246 in each sample was shown in Supplementary Figure 5A. Of the 24 patients, the mean expression level of miR-1246 was 57.5 (/RNU48). We divided those patients into two groups by the mean value of miR-1246 expression (high or low). Disease-free survival ratio (P = 0.0045) and overall survival ratios (P = 0.0102) were significantly lower in the high miR-1246 expression group (Figure 6B).

Subsequently, immunohistochemical staining for CCNG2 was performed in the corresponding 24 samples. The nuclei of normal pancreatic ductal cells were partially stained and the acinar cells were stained strongly in the cytoplasm and nuclei, which were used as positive controls (Supplementary Figure 5B and C). With cancer sections, although CCNG2 had been shown to appear not only in the nucleus but also in the cytoplasm, the functional CCNG2 protein may localise in the nucleus (Choi et al, 2009). We defined CCNG2-positive cases as those that showed diffuse or spotted nuclear patterns (Figure 6C and D), and CCNG2-negative cases as cytoplasmic pattern (not stained in the nucleus; Figure 6E) or an absent pattern (not stained in the nucleus or cytoplasm; Figure 6F) in pancreatic cancer lesions. Among the 24 patients examined, 15 (62.5%) showed positive staining, whereas 9 (37.5%) patients were negative for CCNG2.

Finally, we evaluated the patient backgrounds in low or high miR-1246 expression groups (Table 1 and Supplementary Table 3). The tumour location and CCNG2 expression in other clinico-pathological factors showed significant difference between the two groups. The high miR-1246 expression group showed lower CCNG2 expression, whereas the low miR-1246 expression group showed high CCNG2 expression, with statistical significance (P = 0.047). This result demonstrated that miR-1246 expression correlated inversely with CCNG2 expression in clinical samples, and an especially high expression level of miR-1246 predicted worse pancreatic cancer prognosis.

analysis and GSEA revealed that the stemness-related pathways were increased, suggesting that the spheroids at least partially mimicked the CSC-like phenotype.

miR-1246 was reported as a diagnostic biomarker for oesophageal squamous cell carcinoma (Takeshita et al, 2013) and cervical cancer (Chen et al, 2014). However, few studies have reported the miR-1246 function in pancreatic cancer. In the present study, we demonstrated that miR-1246 induced chemoresistance and was related to cancer stemness in pancreatic cancer cell lines. Among miR-1246 targets, we focused on CCNG2 (Bates et al, 1996), a tumour suppressor gene. The CCNG2 expression was down-regulated in the thyroid (Ito et al, 2003), oral (Kim et al, 2004), breast (Montagner et al, 2012), gastric (Sun et al, 2014a), oesophageal (Chen et al, 2013), prostate (Cui et al, 2014a), kidney (Cui et al, 2014b), and colorectal (Sun et al, 2014b) cancers. Antitumor agents induced CCNG2 expression and inhibited cancer (Kasukabe et al, 2008; Padua and Hansen, 2009; Zhao et al, 2011). We demonstrated that CCNG2 was decreased in pancreatic CSC-like spheroid cells and induced apoptosis, similarly to oral cancer (Kim et al, 2004). Given that CCNG2 deeply participated in cancer proliferation, invasion, chemoresistance, and differentiation, which characterise CSCs, CCNG2 may be involved at least partially in the maintenance of CSC-like spheroid cells. The present data showed CCNG2 expression was correlated inversely with miR-1246 expression, suggesting miR-1246 control CCNG2 function. We confirmed in vitro data by human primary tumours. Laser captured microdissection analysis and immunohistochemistry revealed the high miR-1246 expression and low CCNG2 expression in patients. The present study suggested that miR-1246-CCNG2 axis is critical for chemoresistance, and shows the candidacy as a bona fide useful predictive marker.

DISCUSSION

Several miRNAs were reported in association with drug resistance against GEM: miR-15a (Zhang et al, 2010), miR-21 (Ali et al, 2010; Giovannetti et al, 2010), miR-200b and miR-200c (Ali et al, 2010; Li et al, 2009), miR-320c (Iwagami et al, 2013), and members of the let7 family (Li et al, 2009). Although these reports studied the bulk of tumours, we here identified chemoresistance- and cancer stemness-associated miRNAs. We focused on miR-1246, which was expressed in CSC-like spheroid cells. CSC-like spheroids showed chemoresistance for reagents, and the gene microarray

ACKNOWLEDGEMENTS

REFERENCES

Ali S, Ahmad A, Banerjee S, Padhye S, Dominiak K, Schaffert JM, Wang Z, Philip PA, Sarkar FH (2010) Gemcitabine sensitivity can be induced in pancreatic cancer cells through modulation of miR-200 and miR-21 expression by curcumin or its analogue CDF. *Cancer Res* 70: 3606–3617.

Bartel DP (2009) MicroRNAs: target recognition and regulatory functions. *Cell* 136: 215–233.

Bates S, Rowan S, Vousden KH (1996) Characterisation of human cyclin G1 and G2: DNA damage inducible genes. *Oncogene* 13: 1103–1109.

Chen J, Yao D, Zhao S, He C, Ding N, Li L, Long F (2014) MiR-1246 promotes SiHa cervical cancer cell proliferation, invasion, and migration through suppression of its target gene thrombospondin 2. *Arch Gynecol Obstet* (in press).

Chen JQ, Liu CJ, Wen HX, Shi CL, Zhang HS, Li M, Sun GG (2013) Changes in the expression of cyclin G2 in esophageal cancer cell and its significance. *Tumour Biol* 35: 3355–3362.

Choi MG, Noh JH, An JY, Hong SK, Park SB, Baik YH, Kim KM, Sohn TS, Kim S (2009) Expression levels of cyclin G2, but not cyclin E, correlate with gastric cancer progression. *J Surg Res* 157: 168–174.

Cui DW, Cheng YJ, Jing SW, Sun GG (2014a) Effect of cyclin G2 on proliferative ability of prostate cancer PC-3 cell. *Tumour Biol* 35: 3017–3024.

Cui DW, Sun GG, Cheng YJ (2014b) Change in expression of cyclin G2 in kidney cancer cell and its significance. *Tumour Biol* 35: 3177–3183.

Giovannetti E, Funel N, Peters GJ, Del Chiaro M, Erozenci LA, Vasile E, Leon LG, Pollina LE, Groen A, Falcone A, Danesi R, Campani D, Verheul HM, Boggi U (2010) MicroRNA-21 in pancreatic cancer: correlation with clinical outcome and pharmacologic aspects underlying its role in the modulation of gemcitabine activity. *Cancer Res* 70: 4528–4538.

Hermann PC, Huber SL, Herrler T, Aicher A, Ellwart JW, Guba M, Bruns CJ, Heeschen C (2007) Distinct populations of cancer stem cells determine tumor growth and metastatic activity in human pancreatic cancer. *Cell Stem Cell* 1: 313–323.

Hoyert DL, Heron MP, Murphy SL, Kung HC (2006) Deaths: final data for 2003. *Natl Vital Stat Rep* 54: 1–120.

Ito Y, Yoshida H, Uruno T, Nakano K, Takamura Y, Miya A, Kobayashi K, Yokozawa T, Matsuzuka F, Kuma K, Miyauchi A (2003) Decreased expression of cyclin G2 is significantly linked to the malignant transformation of papillary carcinoma of the thyroid. *Anticancer Res* 23: 2335–2338.

Iwagami Y, Eguchi H, Nagano H, Akita H, Hama N, Wada H, Kawamoto K, Kobayashi S, Tomokuni A, Tomimaru Y, Mori M, Doki Y (2013) miR-320c regulates gemcitabine-resistance in pancreatic cancer via SMARCC1. *Br J Cancer* 109: 502–511.

Kasukabe T, Okabe-Kado J, Honma Y (2008) Cotylenin A, a new differentiation inducer, and rapamycin cooperatively inhibit growth of cancer cells through induction of cyclin G2. *Cancer Sci* 99: 1693–1698.

Kim Y, Shintani S, Kohno Y, Zhang R, Wong DT (2004) Cyclin G2 dysregulation in human oral cancer. *Cancer Res* 64: 8980–8986.

Li C, Heidt DG, Dalerba P, Burant CF, Zhang L, Adsay V, Wicha M, Clarke MF, Simeone DM (2007) Identification of pancreatic cancer stem cells. *Cancer Res* 67: 1030–1037.

Li Y, VandenBoom 2nd TG, Kong D, Wang Z, Ali S, Philip PA, Sarkar FH (2009) Up-regulation of miR-200 and let-7 by natural agents leads to the reversal of epithelial-to-mesenchymal transition in gemcitabine-resistant pancreatic cancer cells. *Cancer Res* 69: 6704–6712.

Lonardo E, Hermann PC, Mueller MT, Huber S, Balic A, Miranda-Lorenzo I, Zagorac S, Alcala S, Rodriguez-Arabaolaza I, Ramirez JC, Torres-Ruiz R, Garcia E, Hidalgo M, Cebrian DA, Heuchel R, Lohr M, Berger F, Bartenstein P, Aicher A, Heeschen C (2011) Nodal/Activin signaling drives self-renewal and tumorigenicity of pancreatic cancer stem cells and provides a target for combined drug therapy. *Cell Stem Cell* 9: 433–446.

Montagner M, Enzo E, Forcato M, Zanconato F, Parenti A, Rampazzo E, Basso G, Leo G, Rosato A, Bicciato S, Cordenonsi M, Piccolo S (2012) SHARP1 suppresses breast cancer metastasis by promoting degradation of hypoxia-inducible factors. *Nature* 487: 380–384.

Oettle H, Post S, Neuhaus P, Gellert K, Langrehr J, Ridwelski K, Schramm H, Fahlke J, Zuelke C, Burkart C, Gutberlet K, Kettner E, Schmalenberg H, Weigang-Koehler K, Bechstein WO, Niedergethmann M, Schmidt-Wolf I, Roll L, Doerken B, Riess H (2007) Adjuvant chemotherapy with gemcitabine vs observation in patients undergoing curative-intent resection of pancreatic cancer: a randomized controlled trial. *JAMA* 297: 267–277.

Padua MB, Hansen PJ (2009) Changes in expression of cell-cycle-related genes in PC-3 prostate cancer cells caused by ovine uterine serpin. *J Cell Biochem* 107: 1182–1188.

Pastrana E, Silva-Vargas V, Doetsch F (2011) Eyes wide open: a critical review of sphere-formation as an assay for stem cells. *Cell Stem Cell* 8: 486–498.

Sun GG, Hu WN, Cui DW, Zhang J (2014a) Decreased expression of CCNG2 is significantly linked to the malignant transformation of gastric carcinoma. *Tumour Biol* 35: 2631–2639.

Sun GG, Zhang J, Hu WN (2014b) CCNG2 expression is downregulated in colorectal carcinoma and its clinical significance. *Tumour Biol* 35: 3339–3346.

Takeshita N, Hoshino I, Mori M, Akutsu Y, Hanari N, Yoneyama Y, Ikeda N, Isozaki Y, Maruyama T, Akanuma N, Komatsu A, Jitsukawa M, Matsubara H (2013) Serum microRNA expression profile: miR-1246 as a novel diagnostic and prognostic biomarker for oesophageal squamous cell carcinoma. *Br J Cancer* 108: 644–652.

Zhang XJ, Ye H, Zeng CW, He B, Zhang H, Chen YQ (2010) Dysregulation of miR-15a and miR-214 in human pancreatic cancer. *J Hematol Oncol* 3: 46.

Zhao Z, Liu Y, He H, Chen X, Chen J, Lu YC (2011) Candidate genes influencing sensitivity and resistance of human glioblastoma to Semustine. *Brain Res Bull* 86: 189–194.

Supplementary Information accompanies this paper on British Journal of Cancer website (http://www.nature.com/bjc)

Combined evaluation of hexokinase 2 and phosphorylated pyruvate dehydrogenase-E1α in invasive front lesions of colorectal tumors predicts cancer metabolism and patient prognosis

Atsushi Hamabe,[1] Hirofumi Yamamoto,[1] Masamitsu Konno,[2] Mamoru Uemura,[1] Junichi Nishimura,[1] Taishi Hata,[1] Ichiro Takemasa,[1] Tsunekazu Mizushima,[1] Naohiro Nishida,[2] Koichi Kawamoto,[1] Jun Koseki,[3] Yuichiro Doki,[1] Masaki Mori[1] and Hideshi Ishii[2,3,4]

Departments of [1]Gastroenterological Surgery; [2]Frontier Science for Cancer and Chemotherapy; [3]Cancer Profiling Discovery, Graduate School of Medicine, Osaka University, Osaka, Japan

Although numerous studies have shown the significance of cancer-specific aerobic glycolysis, how glycolysis contributes to tumor invasion, a critical phenomenon in metastasis, remains unclear. With regard to colorectal cancer (CRC), we studied two critical gate enzymes, hexokinase 2 (HK2), which is involved in glycolysis, and phosphorylated pyruvate dehydrogenase-E1α (p-PDH), which is involved in oxidative phosphorylation (OxPhos). Immunohistochemical analyses using anti-HK2 and p-PDH antibodies were performed on surgically resected CRC samples ($n = 104$), and the expression in invasive front lesions of tumors was assessed. Positive HK2 expression correlated with extensive tumor diameter ($P = 0.0460$), advanced tumor depth ($P = 0.0395$), and presence of lymph node metastasis ($P = 0.0409$). Expression of p-PDH tended to be higher in right-sided CRCs than in left-sided CRCs ($P = 0.0883$). In survival analysis, the combined evaluation of positive HK2 and negative p-PDH was associated with reduced recurrence-free survival (RFS) ($P = 0.0169$ in all stages and $P = 0.0238$ in Stage II and III patients, respectively). This evaluation could predict RFS more precisely than the independent evaluation. The present study indicated that high HK2 expression combined with low p-PDH expression in the invasive front lesions of CRC tumors is predictive of tumor aggressiveness and survival of CRC cases.

C olorectal cancer (CRC) is the second most common cancer in the world. Each year, >1.2 million individuals develop CRC, and approximately 600 000 deaths occur.[1] Although the efficacy of treatment has been gradually improving because of advances in chemotherapy or surgical technologies, the prognosis of patients with distant metastases and recurrence has not improved much. Numerous studies have shown that the activation of tumor-promoting genes and inactivation of growth-constraint tumor suppressor genes through genetic and epigenetic alterations contribute to the activation of biological phenomena, such as cell invasion, movement, and colonization, in distant organs during the metastatic process[2,3]; however, the precise molecular mechanisms involving biologically active metabolites in cancer are not completely understood.

Recent studies have indicated that deregulation in intratumor metabolism is involved in malignant behaviors of cancer cells.[4,5] In glucose metabolism, lactate is preferentially produced in cancer cells, even in the presence of adequate oxygen in culture, a critical biological phenomenon termed aerobic glycolysis or the Warburg effect.[6] Pyruvate kinase M2 (PKM2) was identified as a key molecule involved in the Warburg effect.[7] Subsequently, at least three other enzymes, including phosphofructokinase 1, hexokinase 2 (HK2), and a phosphorylated form of pyruvate dehydrogenase-E1α (p-PDH), have been shown to be involved in cancer-associated metabolism, including glycolysis and oxidative phosphorylation (OxPhos) in the mitochondria.[8–10] Aerobic glycolysis is thought to be beneficial for the production of biomass, such as nucleic acids and lipids, and reduced forms of glutathione, thereby conferring the advantages of low oxidative stress and selective growth.

In the initial step of glycolysis, HK converts glucose and ATP to glucose-6-phosphate and ADP. Four HK isoforms, HK1, HK2, HK3, and HK4, which are encoded by separate genes,[11] are expressed in mammals. In adult tissues, HK1 is

ubiquitously expressed, whereas HK2 is expressed in limited types of tissues, such as adipose tissues, skeletal muscles, and the heart.[12] In cancer cells, HK2 and, to a lesser extent, HK1 are expressed,[13] which suggests a preferential role of HK2 in the glucose flux of cancer cells. Recent studies have indicated that HK2 is necessary for the tumorigenicity of non-small cell lung cancer and breast cancer in humans, whereas HK2 deletion results in rapid suppression of tumor growth.[9]

Pyruvate dehydrogenase has a gate-keeper role in a branching point that links glycolysis to OxPhos in the citric acid cycle by converting pyruvate to acetyl-CoA in the mitochondria. The catalyzing activity of PDH is inhibited by phosphorylation at serine residue(s) by PDH kinase (PDK), whereas PDH is activated by PDH phosphatase.[14,15] Reportedly, the process of aerobic glycolysis is at least partially maintained by the attenuation of mitochondrial function through PDH inhibition.[16] A melanoma study showed that PDH inactivation by serine 293-phosphorylation by PDK led to high tumorigenic activity, whereas PDK depletion resulted in hypophosphorylation of PDH, regression of tumors, and further eradication of subpopulations resistant to a specific inhibitor to oncogene BRAF,^{V600E}[17] which suggested an exclusive dependency on aerobic glycolysis of melanoma growth.

In the present study, we immunohistochemically analyzed the expression of HK2 and p-PDH in the invasive front lesions of clinical CRC samples and assessed their ability to predict tumor aggressiveness and survival. We identified an unexpected association of p-PDH with improved survival and showed that combined expression of HK2 and p-PDH was predictive of patient survival. Furthermore, we induced epithelial–mesenchymal transition (EMT) to colon cancer cell, followed by biochemical assays of HK and PDH. These results suggest a unique role of p-PDH in CRC growth at invasive fronts.

Materials and Methods

Clinical tissue samples. Colorectal tissue samples (*n* = 104) were collected during surgery (2007–2009) at the Department of Surgery, Osaka University. None of the patients had undergone preoperative chemotherapy or irradiation. Samples were fixed in buffered formalin at 4°C overnight, processed through graded ethanol solutions, and embedded in paraffin. The specimens were appropriately used under the approval of the ethics committee at the Graduate School of Medicine, Osaka University.

Immunohistochemistry. Tissue sections (3.5 μm thick) were prepared from paraffin-embedded blocks. After antigen retrieval treatment in 10 mM citrate buffer (pH 6.0) at 115°C for 15 min using Decloaking Chamber NxGen (Biocare Medical, Concord, CA, USA), immunostaining was performed using the Vectastain ABC Peroxidase Kit (Vector Laboratories, Burlingame, CA, USA). Antibodies used for immunohistochemistry were anti-HK2 rabbit antibody (2867; Cell Signaling Technology, Danvers, MA, USA), anti-pyruvate dehydrogenase E1α subunit (PDH-E1α) mouse antibody (ab110330; Abcam, Cambridge, UK), and pSer293 (p-PDH), the anti-phosphorylated form of PDH-E1α rabbit antibody (AP1062; Millipore, Darmstadt, Germany). The specificity of the antibodies was confirmed by the data showing that each antibody detected single band corresponding to the targeted protein in Western blot analysis (Suppl. Figs S1–3), and additionally, in regard to HK2 antibody, the absorption test was carried out in immunohistochemical analysis (Suppl. Fig. S4). The slides were incubated overnight at 4°C at the following dilutions: anti-HK2 antibody, 1:200; anti-p-PDH, 1:500; anti-PDH-E1α, 1:200.

Sections were counterstained with hematoxylin. We rated the intensity of staining on a scale of 0 to 2: 0, negative; 1, weak; and 2, strong. We used pancreatic tissue as a positive control of HK2 according to the previous study,[18] and a case of Stage I rectal cancer, the staining of which at the deepest part was strong as a positive control of p-PDH. Phosphate buffered saline instead of the antibodies was used as a negative control. We assigned colorectal tissue stained as intense as the positive control to "intensity score 2", while unstained colorectal tissue similar to the negative control was assigned to "score 0" (Fig. 1). The tissue stained weaker than the positive control but stronger than the negative control was categorized into "score 1" (Fig. 1b,c). The intensity at the deepest part of the tumor was recorded in each sample. The reason why the intensity at the deepest part of the tumor was assessed was that the cancer cell was stimulated to invade into surrounding tissues at this region.[19,20]

Assessment of tumor budding. Tumor budding was estimated according to the definition proposed by Ueno et al.[21,22] An isolated cancer cell or a cluster composed of fewer than five cancer cells was defined as tumor budding. The number of buddings was counted in the field under a magnification of ×200 in the invasive front area.

Cell lines and culture. Human colon cancer cell line, SW480, was obtained from the ATCC (Manassas, VA, USA). The cells were grown in Dulbecco's modified Eagle's medium (DMEM) supplemented with 10% FBS, 100 U/mL penicillin, and 100 U/mL streptomycin, and grown at 37°C in a humidified incubator with 5% CO_2.

Induction of EMT. Cells were seeded at the concentration of 5.0×10^4 cells/mL and incubated in a humidified atmosphere (37°C and 5% CO_2) in standard medium for 48 h. After 48 h incubation, the cells were treated with transforming growth factor-β1 (TGF-β1) (2.5 ng/mL) and were incubated with MEM medium supplemented with FBS free, 10 ng/mL epidermal
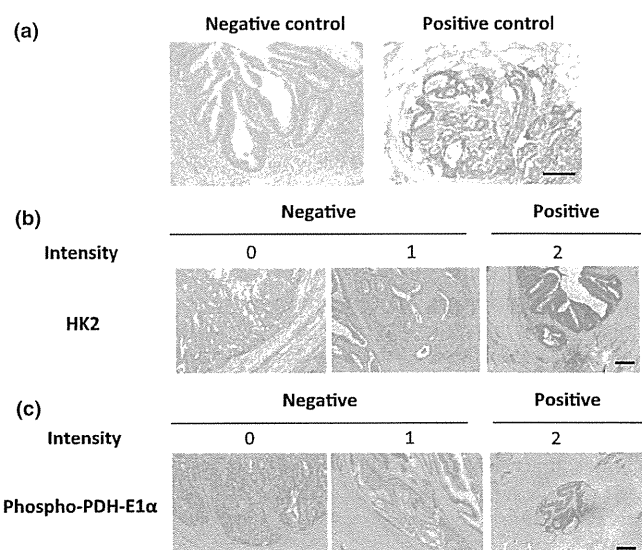

Fig. 1. Immunohistochemical analysis of HK2 and p-PDH in clinical colorectal cancer samples. (a) Phosphate buffered saline was used as a negative control and a case of pancreatic cancer tissue was used as a positive control for HK2. (b) Staining of HK2 and (c) p-PDH at the invasive front are shown; the intensity was rated in three stages. Scale bar, 200 μm.

growth factor (Sigma-Aldrich, St Louis, MO, USA), 100 × insulin/transferring/selenium (ITS) (Life Technologies, Carlsbad, CA, USA), and 50 nmol/L hydrocortisone (Tokyo Kasei, Tokyo, Japan) for 48–72 h.

Biochemical assay. Biochemical activities of SW480 were analyzed using Hexokinase Colorimetric Assay Kit (ab136957; Abcam) for hexokinase activity and Pyruvate dehydrogenase Enzyme Activity Microplate Assay Kit (ab109902; Abcam) for pyruvate dehydrogenase activity according to the manufacturer's instructions.

Western blot analysis. Total protein was extracted from the cell lines in radio immunoprecipitation assay (RIPA) buffer (Thermo Fisher Scientific, Rockford, IL, USA). Aliquots of protein were electrophoresed on SDS-PAGE, Tris-HCl gels (Bio-Rad Laboratories, Hercules, CA, USA). The separated proteins were transferred to PVDF membranes using iBlot (Life Technologies). Antibodies specific to E-cadherin (3195; Cell Signaling Technology), Vimentin (5741; Cell Signaling

Technology), ACTB (A2103, Sigma-Aldrich) were used in addition to the antibodies used for immunohistochemistry. The membranes were incubated with primary antibodies overnight at 4°C, at appropriate concentrations (1:1000 for E-cadherin; 1:1000 for Vimentin; 1:1000 for HK2; 1:1000 for PDH-E1α; 1:10 000 for p-PDH; 1:2000 for ACTB) followed by the incubation with horseradish-peroxidase-linked anti-rabbit or mouse IgG (GE Healthcare Biosciences, Piscataway, NJ, USA) at a dilution of 1:100 000 for 1 h at room temperature. The antigen–antibody complex was detected with the ECL Prime Western Blotting Detection Kit (GE Healthcare Biosciences).

Quantitative reverse transcription polymerase chain reaction. Total RNA was extracted from cultured cells using RNeasy Mini Kit and QIA shredder (Qiagen, Valencia, CA, USA). Complemetary DNA was synthesized with ReverTra Ace reverse transcriptase (Toyobo, Osaka, Japan). Real-time quantitative polymerase chain reactions (qRT-PCR) were conducted with the LightCycler-FastStart DNA Master SYBR

Table 1. HK 2 expression and clinicopathological features of colorectal cancer

Hexokinase 2	Positive (n = 61)	Negative (n = 43)	P-value
Patient background			
Gender (Male/Female)	37/24	28/15	0.6436
Age (mean ± SD)	63.2 ± 12.4	66.6 ± 10.6	0.9265
BMI (kg/m^2)	22.2 (20.5, 26.1)	22.4 (20.3, 25.2)	0.9579
CEA (ng/mL)	3 (2, 9)	3 (1, 5)	0.5232
CA19-9 (U/mL)	11 (7, 21)	13 (5, 22)	0.8013
Tumor characteristics			
Tumor diameter (mm)	40 (25, 54)	30 (20, 44)	0.0460*
Location			
C/A/T	5/10/7	3/5/7	0.9013
D/S/R	2/13/24	2/7/19	
Tumor type			
Type 0	13	13	0.3008
Type 1/2/3/4/5	3/32/12/0/1	3/22/4/0/1	
Histological type			
tub1/tub2/pap	17/39/1	13/23/1	0.3118
por/muc	0/4	4/2	
Depth			
T0/T1/T2	5/5/13	3/10/12	0.0395*
T3/T4	31/7	15/3	
Lymph node metastasis			
N0	35	33	0.0409*
N1/N2/N3	16/7/3	7/0/3	
Distant metastasis			
M0	53	40	0.5190
M1	8	3	
Lymphatic duct invasion			
ly0	15	19	0.2321
ly1/ly2	34/12	21/3	
Venous invasion			
v0	48	36	0.6176
v1/v2	9/4	7/0	
Stage			
0/I/II	5/13/15	3/20/9	0.0350*
IIIa/IIIb/IV	13/7/8	6/2/3	

*Statistically significant. Data are presented as median (first quartile, third quartile). A, ascending colon; BMI, body mass index; C, cecum; D, descending colon; muc, mucinous carcinoma; pap, papillary adenocarcinoma; por, poorly differentiated adenocarcinoma; R, rectum; S, sigmoid colon; T, transverse colon; tub1, well-differentiated adenocarcinoma; tub2, moderately differentiated adenocarcinoma.

Table 2. p-PDH expression and clinicopathological features of colorectal cancer

Phospho-PDH-E1α	Positive (n = 34)	Negative (n = 70)	P-value
Patient background			
Gender (Male/Female)	22/12	43/27	0.7461
Age (mean ± SD)	66.0 ± 10.4	63.5 ± 13.3	0.1669
BMI (kg/m^2)	23.6 (20.6, 25.6)	21.9 (20.3, 25.6)	0.4316
CEA (ng/mL)	2.5 (1, 6)	3 (2.0, 7.3)	0.4401
CA19-9 (U/mL)	12.5 (5.0, 23.3)	12.5 (7.0, 21.3)	0.8538
Tumor characteristics			
Tumor diameter (mm)	37 (22, 52)	35 (22, 52)	0.6126
Location			
C/A/T	5/6/5	3/9/9	0.0883
D/S/R	3/3/12	1/17/31	
Tumor type			
Type 0	11	15	0.2275
Type 1/2/3/4/5	1/16/4/0/2	5/38/12/0/0	
Histological type			
tub1/tub2/pap	10/18/1	20/44/1	0.2893
por/muc	2/3	2/3	
Depth			
T0/T1/T2	3/4/7	5/11/18	0.4779
T3/T4	16/4	30/6	
Lymph node metastasis			
N0	23	45	0.7354
N1/N2/N3	5/4/2	18/3/4	
Distant metastasis			
M0	29	64	0.3339
M1	5	6	
Lymphatic duct invasion			
ly0	12	22	0.6857
ly1/ly2	15/7	40/8	
Venous invasion			
v0	26	58	0.4394
v1/v2	7/1	9/3	
Stage			
0/I/II	3/9/10	5/24/14	0.7461
IIIa/IIIb/IV	4/3/5	15/6/6	

Data are presented as median (first quartile, third quartile). A, ascending colon; BMI, body mass index; C, cecum; D, descending colon; muc, mucinous carcinoma; pap, papillary adenocarcinoma; por, poorly differentiated adenocarcinoma; R, rectum; S, sigmoid colon; T, transverse colon; tub1, well-differentiated adenocarcinoma; tub2, moderately differentiated adenocarcinoma.

Green I kit (Roche Applied Science, Basel, Switzerland). The primer sequences used in this study were: HK2 sense, 5′-CA-AAGTGACAGTGGGTGTGG-3′; HK2, antisense, 5′-GCCAG GTCCTTCACTGTCTC-3′; PDK1 sense, 5′-CCAAGACCTCG TGTTGAGACC-3′; PDK1 antisense, 5′-AATACAGCTTCAG GTCTCCTTGG-3′; PDP2 sense, 5′-ACCACCTCCGTGTCTA TTGG-3′; PDP2 antisense, 5′- CCAGCGAGATGTCAGAATC C-3′. Data were normalized to expression of a control gene (b-actin) for each experiment. Data represent the mean ± SD of three independent experiments.

Statistical analysis. JMP pro 10.0.2 software (SAS Institute, Cary, NC, USA) was used to perform statistical analysis. The Kaplan–Meier method was used to estimate tumor recurrence in CRC, and the log-rank test was used to determine the statistical significance. Associations between discrete variables were assessed using the χ^2 test or Fisher's exact test as appropriate. Mean values were compared using the Mann–Whitney U-test. P-values <0.05 were considered to indicate statistical significance.

Results

HK2 in CRC. We performed immunohistochemical staining of HK2 in clinical samples of CRCs. The intensities of HK2 staining rated in three stages were assigned to two groups: the HK2-negative group included scores of 0 or 1, while the HK2-positive group included score of 2 (representative cases are shown in Fig. 1b). As summarized in Table 1, HK2 expression was significantly associated with extensive tumor diameter ($P = 0.0460$), advanced tumor depth ($P = 0.0395$), and positive lymph node metastasis ($P = 0.0409$), suggesting that the HK2-positive group had more patients with advanced stages than the HK2-negative group. HK2 expression was not associated with the backgrounds of the patients, including serum tumor markers, tumor locations, and histological types of tumors.

p-PDH in CRCs. Immunohistochemical staining of p-PDH was performed in a manner similar to that of immunohistochemical analysis of HK2 (Fig. 1c). Correlations between p-PDH expression and clinicopathological factors are summarized in Table 2. In contrast to HK2 expression, p-PDH expression did not show any correlations with tumor depth, lymph node metastasis, or other patient backgrounds. Assessment of tumor locations indicated that p-PDH expression tended to be higher
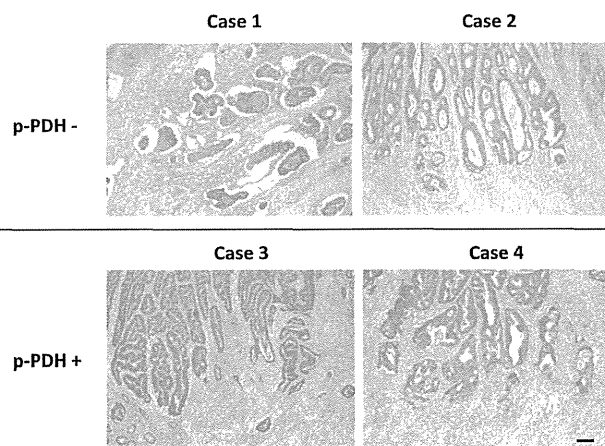
Table 3. Correlation between the immunohistochemical staining of phosphorylation status of PDH-E1α

	p-PDH		
	Positive	Negative	*P*
Total PDH-E1α			
Positive	6	8	1.0000
Negative	2	3	

in right-sided CRCs than in left-sided CRCs, but did not reach statistical significance. We also performed immunohistochemical analysis to detect the total amount of PDH-E1α regardless of phosphorylation status in 19 colorectal cancer tissues. The result showed that total PDH-E1α-positive cases showed p-PDH positive or negative expression (Fig. 2; Figs S2 and S3), whereas the total PDH-E1α-negative cases (intensity score 0) was absent for p-PDH expression, although the low expression cases (score 1) could be p-PDH positive (Table 3; data not shown), suggesting that the phosphorylation event is independent of the protein amount, and that phosphorylation control may be critical in clinical status of tumors.

Heterogeneity of HK2 or p-PDH staining in CRC and in normal mucosa. We examined whether the heterogeneity of HK2 or p-PDH staining in CRC might be observed, and moreover, the staining intensities in normal mucosa. As shown in Table 4, positive correlation could be observed between the staining intensities in the deep part and in the superficial part of tumors regarding HK2 and p-PDH expression. In relation to the expression in normal mucosa, both expressions could scarcely be observed and any correlations with the staining in the deep part of tumor could not be observed.

Recurrence-free survival. We studied the correlations of HK2 or p-PDH expression with recurrence-free survival (RFS) in all the patients except for nine Stage IV patients who underwent non-curable resection. HK2 could separate the patients by prognosis, with positive HK2 expression being associated with

Table 4. Assessment of the staining heterogeneity of HK2 and p-PDH in tumor superficial and deep part and in normal mucosa

	HK2 staining in deep part		
	Positive	Negative	*P*
HK2 staining in superficial part			
Positive	30	10	0.0074*
Negative	31	33	
HK2 staining in normal mucosa			
Positive	1	1	1.0000
Negative	54	38	

	p-PDH staining in deep part		
	Positive	Negative	*P*
p-PDH staining in superficial part			
Positive	28	36	0.0024*
Negative	6	34	
p-PDH staining in normal mucosa			
Positive	0	0	NA
Negative	31	66	

Fig. 2. Immunohistochemical analysis of PDH-E1α. Representative images of PDH-E1α staining in p-PDH negative cases (case 1 and 2) and p-PDH positive cases (cases 3 and 4). Scale bar, 100 μm.

*Statistically significant. In the assessment of staining in normal mucosa, the cases that did not contain normal mucosa in paraffin section were not included.
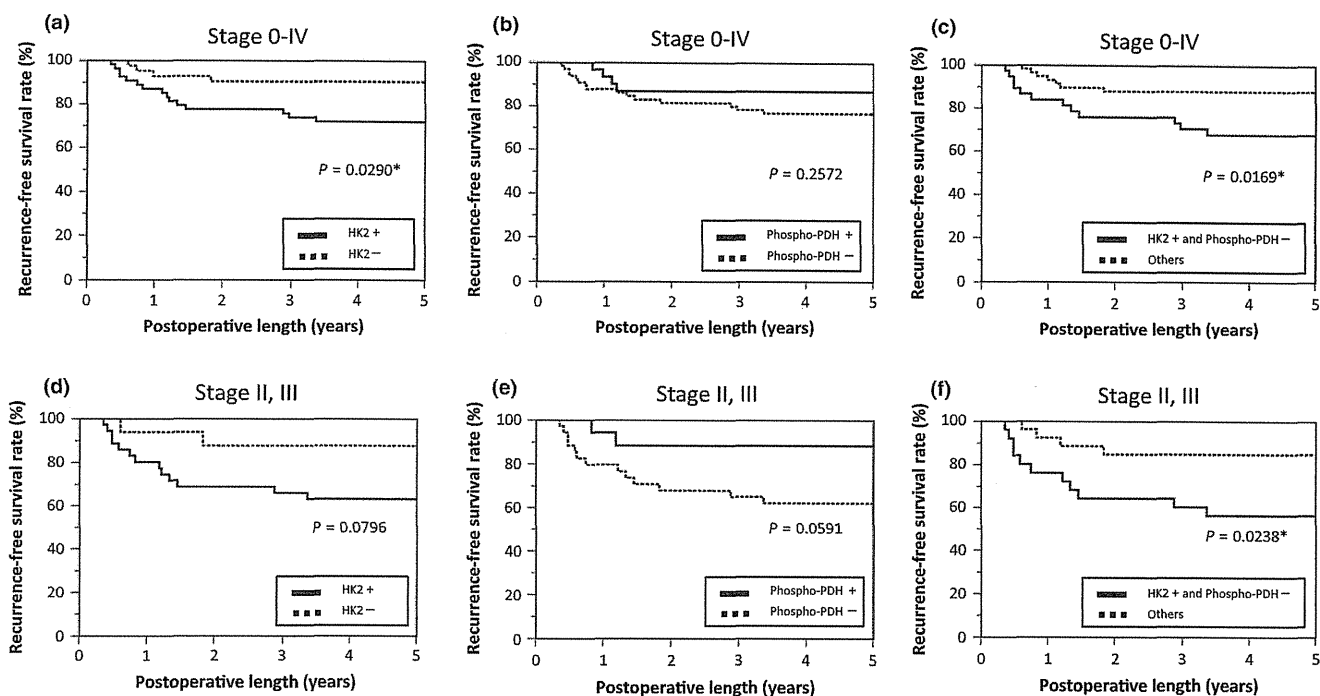
Fig. 3. Recurrence-free survival curves of the analyzed patients. (a) Patients in all stages were analyzed based on the level of HK2 expression. (b) Patients in all stages were analyzed based on the level of p-PDH expression. (c) Patients in all stages were analyzed based on combined expression of HK2 and p-PDH. (d) Patients in stage II and III were analyzed based on the level of HK2 expression. (e) Patients in stage II and III were analyzed based on the level of p-PDH expression. (f) Patients in stage II and III were analyzed based on combined expression of HK2 and p-PDH. *Statistically significant.

a poor survival rate ($P = 0.0290$) (Fig. 3a). In contrast, negative p-PDH expression tended to correlate with poor RFS, but this difference was not statistically significant ($P = 0.2572$)

(Fig. 3b). We then assessed the ability of the combination of two metabolic markers to predict aggressive phenotypes of tumors and survival of patients. We classified the patients into

Table 5. Results of univariate and multivariate Cox regression analysis for Stage 0–IV patients

Variables	Univariate		Multivariate	
	HR (95% CI)	P	HR (95% CI)	P
Age	1.017 (0.977–1.063)	0.4066		
Gender				0.0120*
Female	Reference			
Male	3.015 (1.004–12.963)	0.0491*	4.186 (1.365–18.220)	
Tumor diameter	1.014 (0.994–1.032)	0.1515		
Location				
Right-sided	Reference	0.2371		
Left-sided	1.806 (0.691–5.588)			
Tumor type				
Type 0	Reference	0.0062*		
Type 1/2/3/4/5	7.787 (1.608–140.039)			
Histological type				
tub1/tub2/pap	Reference	0.5763		
por/muc	1.557 (0.247–5.434)			
Depth				
T0/T1/T2	Reference	0.0028*		0.0162*
T3/T4	4.497 (1.631–15.781)		3.695 (1.257–13.500)	
Lymph node metastasis				
N0	Reference	0.0009*		0.0190*
N1/N2/N3	4.716 (1.892–12.704)		3.156 (1.207–8.912)	
Immunohistochemistry				
Others	Reference	0.0198*		0.0656
HK2+ and p-PDH-	2.952 (1.187–7.933)		2.383 (0.946–6.475)	

*Statistically significant. CI, confidence interval; HR, hazard ratio.

Table 6. Results of immunohistochemistry for Stage II and III cases based on HK2 and p-PDH expression

	HK2 expression	
	Positive	Negative
p-PDH expression		
Positive	10	6
Negative	25	11

two groups: the combined HK2-positive and p-PDH-negative group and the group consisting of the other cases. This immunohistochemical evaluation of combined enzyme expression showed that positive HK2 expression combined with negative p-PDH expression was associated with poor RFS rates ($P = 0.0169$), which could be considered as more sensitive prognostic factor than HK2 alone (Fig. 3a–c). In the multivariate analysis, tumor depth and lymph node metastasis were found to be independent prognostic factors, while the combined evaluation showed the statistical significance in univariate, but not in multivariate analysis (Table 5).

Furthermore, we carried out a similar analysis of RFS for the 52 patients, including 24 Stage II patients and 28 Stage III patients, who had a certain level of recurrence risk and might benefit from adequate estimation of recurrence risk in that the necessity of adjuvant therapy could be evaluated (Table 6).[23] HK2 and p-PDH expression tended to separate the patients by prognosis; however, significant differences were not observed ($P = 0.0796$ and 0.0591, respectively; Fig. 3d,e). Interestingly, the immunohistochemical evaluation of combined enzyme expression showed that positive HK2 expression combined with negative p-PDH expression significantly correlated with poor RFS rates ($P = 0.0238$) (Fig. 3f). Multivariate analysis showed the combination of positive HK2 and negative p-PDH

expression was independently associated with poor prognosis ($P = 0.0389$) (Table 7).

Budding. To confirm the reason why the combined evaluation of both HK2 and p-PDH expression strongly correlated with RFS in colorectal cancer patients especially in Stage II and III, we analyzed the association between the combined evaluation and "budding". As a result, positive HK2 and negative p-PDH associated with the increased number of budding ($P = 0.0199$) (Fig. 4).

HK2 and PDH activity analysis. In the process of invading into stroma, cancer cells acquire the ability to detach from the epithelial lining and migrate, which is regulated by the mechanism of EMT, in a manner similar to the developmental program of an embryo. A set of pleiotropically acting genes orchestrates the EMT process by evoking loss of adherent junctions, conversion to spindly shapes, increased motility, and resistance to apoptosis in invasive front lesions of tumors.[24] To study the underlined mechanism in the present observation, we induced EMT to colon cancer cell line SW480, as a model of invading colorectal cancer cells, according to the previously described procedure followed by the analyses of HK and PDH activity.[25–28] In response to EMT stimulation, cell morphology changed from epithelial to fibroblastic-like spindle shape (Fig. 5a) and expression of E-cadherin was decreased and Vimentin was increased (Fig. 5b). By acquiring mesenchymal phenotype, HK2 expression and phosphorylation level of PDH were up-regulated (Fig. 5b). Corresponding to these shifts in the expression of the two enzymes, HK activity and PDH activity were augmented in biochemical analyses (Fig. 5c,d). Activity of PDH is regulated by two key PDH-modifying enzymes; PDK1 phosphorylates PDH to suppress the function, whereas PDP2 dephosphorylates PDH to stimulate it.[17] We found that PDP2 expression was increased in EMT condition, but PDK1 expression was stable, which might explain why p-PDH was down-regulated (Fig. 5e).

Table 7. Results of univariate and multivariate Cox regression analysis for Stage II and III patients

Variables	Univariate		Multivariate	
	HR (95% CI)	*P*	HR (95% CI)	*P*
Age	1.026 (0.976–1.077)	0.3052		
Gender				
Female	Reference	0.0166*		0.0270*
Male	4.657 (1.284–29.806)		4.740 (1.175–32.086)	
Tumor diameter	1.011 (0.989–1.030)	0.3140		
Location				
Right-sided	Reference	0.0974		0.9038
Left-sided	2.496 (0.8526–9.011)		0.923 (0.270–3.821)	
Histological type				
tub1/tub2/pap	Reference	0.8206		
por/muc	1.193 (0.186–4.321)			
Depth				
T0/T1/T2	Reference	0.3387		
T3/T4	2.390 (0.4803–43.287)			
Lymph node metastasis				
N0	Reference	0.0813		0.1745
N1/N2/N3	2.616 (0.892–9.458)		2.284 (0.705–8.957)	
Immunohistochemistry				
Others	Reference	0.0230*		0.0389*
HK2+ and p-PDH-	3.451 (1.179–12.463)		3.143 (1.058–11.461)	

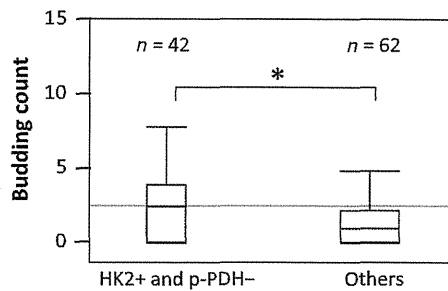*Statistically significant. CI, confidence interval; HR, hazard ratio.

Fig. 4. The budding count in colorectal cancer tissues. The budding count of HK2+ and p-PDH- cancers was significantly greater than that of the others ($P = 0.0199$). *Statistically significant.

Discussion

An increasing amount of evidence has shown that cancer-specific alterations in metabolism, that is, enhanced glucose uptake and successive preferential conversion to lactate, are important factors in cancer metabolism (the Warburg effect)[6,29] and constitute tumor growth. This system is beneficial for the biosynthetic and bioenergetic demands of proliferation by diverting glycolytic intermediates to an alternative biosynthetic, the pentose phosphate pathway. Moreover, these metabolic systems are attractive targets for possible therapeutic interventions and currently research is ongoing to demonstrate the definite mechanism of cancer metabolism.[30] Although aerobic glycolysis is intimately linked to tumor growth and cancer cell proliferation, how glycolysis is involved in cellular invasion remains unclear. Invasion and metastasis are hallmarks of cancer and are closely associated with the development of pathological stages of cancer arising from precancerous lesions in epithelial tissues.[24] Distant metastasis becomes clinically evident as a consequence of multistep cascades that initially occur in local invasions.[31,32] Thus, the study of the effect of cancer metabolism in invasion may be beneficial for elucidating the novel mechanism of invasion and metastasis. To the best of our knowledge, this is the first study to demonstrate a significant association between the expression of the biomarkers HK2 and p-PDH and patient survival.

Although tumor heterogeneity is largely a common feature for the generation of biological plasticity, genetic diversification,
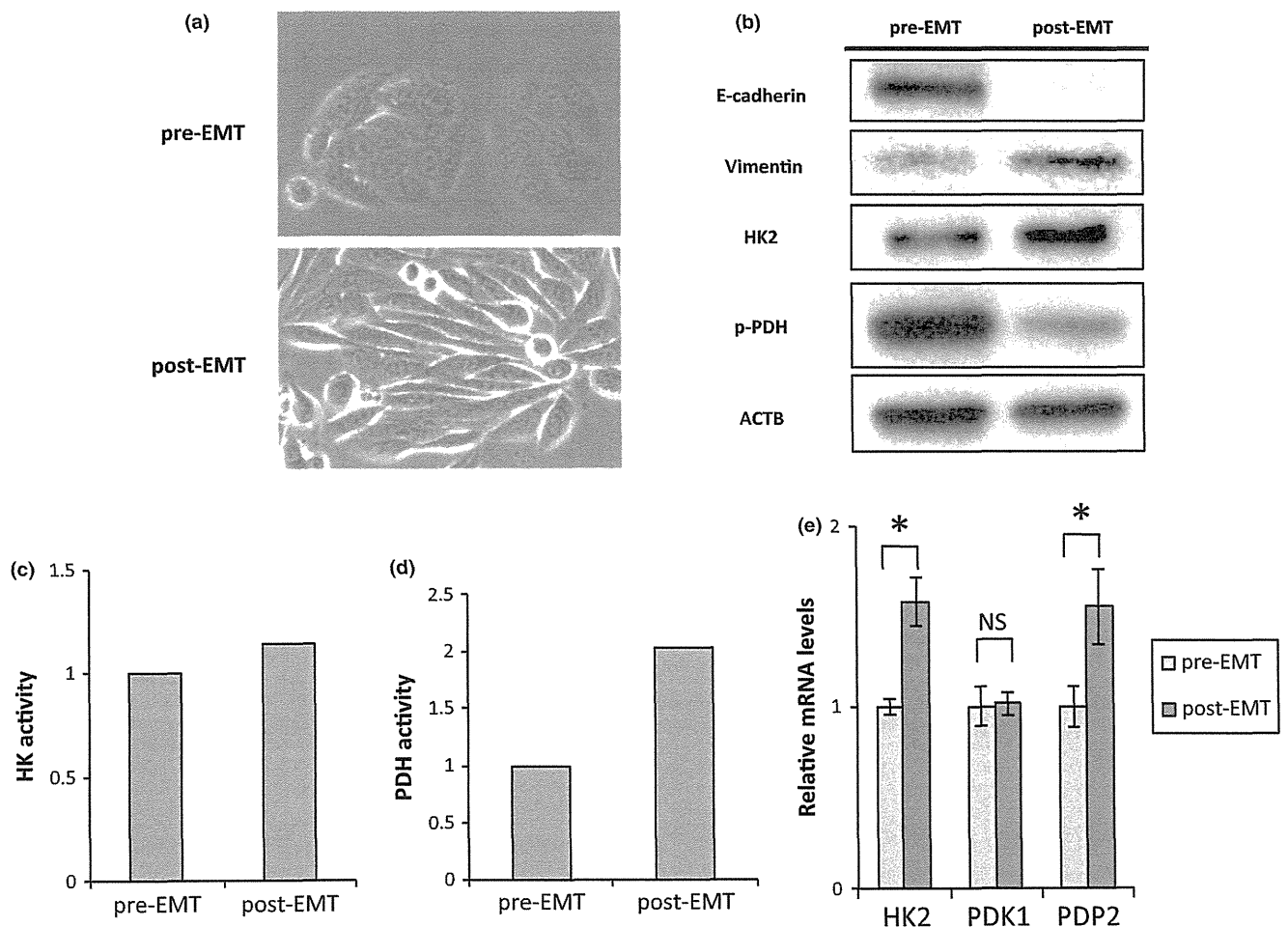

Fig. 5. Epithelial–mesenchymal transition (EMT) accompanies HK2 upregulation and p-PDH downregulation. (a) Photomicrographs of the morphological change of SW480 cells. (b) Western blot assays of E-cadherin, Vimentin, HK2, p-PDH, and ACTB expression in pre-EMT and post-EMT cells. Samples of post-EMT cells were harvested at 72 h. (c) Hexokinase activity in pre-EMT and post-EMT cells. Samples of post-EMT cells were harvested at 72 h. (d) Pyruvate dehydrogenase activity in pre-EMT and post-EMT cells. Samples of post-EMT cells were harvested at 72 h. (e) Relative transcript (mRNA) levels of HK2, PDK1, and PDP2 after inducing EMT for 0 and 48 h. The values at 0 h have been normalized to 1, and the data are expressed as fold. *Statistically significant.